Validity of the sonar equation and Babinet's principle for scattering in a stratified medium

Purnima Ratilal, Yisan Lai, and Nicholas C. Makris[a)]

Massachusetts Institute of Technology, Cambridge, Massachusetts 02139

The sonar equation rests on the assumption that received sound pressure level after scattering can be written in decibels as a sum of four terms: source level, transmission loss from the source to the target, target strength, and transmission loss from the target to the receiver. This assumption is generally not valid for scattering in a shallow water waveguide and can lead to large errors and inconsistencies in estimating a target's scattering properties as well as its limiting range of detection. By application of coherent waveguide scattering theory, the sonar equation is found to become approximately valid in a shallow water waveguide when the object's complex scatter function is roughly constant over the equivalent horizontal grazing angles $\pm\Delta\psi$ spanned by the dominant waveguide modes. This is approximately true (1) for all objects of spatial extent L and wavelength λ when $2\Delta\psi < \lambda/2L$ and (2) for spheres and certain other rounded objects in nonforward scatter azimuths, even when (1) does not hold. The sonar equation may be made valid by lowering the active frequency of operation in a waveguide. This is often desirable because it greatly simplifies the analysis necessary for target classification and localization. Similarly, conditions are given for when Babinet's principle becomes approximately valid in a shallow water waveguide. © *2002 Acoustical Society of America.* [DOI: 10.1121/1.1499136]

PACS numbers: 43.30.Ft, 43.30.Gv, 43.30.Vh [DLB]

I. INTRODUCTION

The sonar equation is the most widely used analytical tool in applications of active sonar.[1–5] It is typically employed to estimate a target's scattering properties and limiting range of detection.[1] The sonar equation, in its active form for an omnidirectional source, rests on the assumption that received sound pressure level in decibels can be written as a sum of four terms: source level, transmission loss from the source to the target, target strength, and transmission loss from the target to the receiver. This assumption has two related implications: (1) that propagation and scattering effects are completely factorable from each other, and (2) that a linear combination of the incoherent quantities, target strength, transmission loss, and source level completely specifies the sound pressure level at the receiver.

When this assumption is axiomatically adopted in an ocean waveguide, fundamental inconsistencies can occur when experimental data is examined. For example, the target strength of an object, which should be invariant, can vary significantly with range when experimentally estimated in a range-independent environment where the direct return arrives together with multiple returns from the waveguide boundaries. This has been noted in the classic text, *Physics of Sound in the Sea*.[2] Regardless of this inconsistency, target strength is still used in that text to describe the scattering properties of an object because a more fundamental approach had not presented itself, just as it is still used today by many practitioners of ocean acoustics.

Our goal in the present paper is to (1) demonstrate that the assumption that the sonar equation rests on and its implications are not generally valid for scattering in a shallow water waveguide, and (2) provide conditions necessary for the sonar equation to become valid in a shallow water waveguide.[6] In the process we show that the invariant scattering properties of an object in a waveguide cannot generally be described by target strength, an incoherent quantity, but rather require a coherent representation that arises from the fundamental waveguide scattering theory[7,8] upon which our analysis is based.

First developed in World War II,[1,2] the sonar equation, analogous to the radar equation, *is only valid when propagation and scattering dependencies are approximately separable.* For example, given an omnidirectional point source and receiver in free space, propagation and scattering are separable when the source and receiver are in the farfield of the target, where the incident as well as the scattered wave may be approximated as planar. The sonar equation has a long history of legitimate usage in deep water,[1,2] where these free-space conditions are effectively achieved in many practical scenarios due to the significant time separation that often occurs between direct and surface reflected arrivals and the adiabatic nature of refraction in the ocean.

In continental shelf environments, referred to as shallow water waveguides in ocean acoustics, multiple reflections from the surface and bottom typically overlap and *coherently* interfere with each other and the direct arrival. No unique incident and scattered angle exists. To understand the implications for scattering, it is convenient to decompose the incident field at a target in a waveguide from a farfield point

[a)]Electronic mail: makris@mit.edu

source, into modal plane waves. Each incident plane wave arrives with a specific elevation angle from the azimuth of the farfield source and then scatters *coherently* from the target into outgoing plane waves in all elevation and azimuthal angles. The target affects both the amplitude and phase of each scattered plane wave. *This phase change cannot be described by an incoherent quantity such as target strength.* At a farfield receiver, the scattered field is the *coherent* sum of all scattered plane waves from all incident plane waves. Just as waveguide propagation models must account for the *coherent* interference of multiple arrivals from a source to receiver to accurately determine transmission loss, waveguide scattering models must account for the *coherent* interference of all scattered waves from every wave incident on the target. Propagation and scattering are in this way *coherently* convolved for objects submerged in a waveguide.

To establish when the sonar equation can be applied in a shallow water waveguide, we calculate the scattered field from a variety of target types in various shallow water waveguides using a physics-based waveguide scattering model[7,8] that takes into account the coupling between propagation and scattering. We then compare the results to those predicted by the sonar equation. The waveguide scattering model, based on Green's Theorem, expresses the scattered field in terms of normal modes, convenient for long-range propagation, and the plane wave scatter function of the object. The only assumptions needed for the waveguide scattering model to be valid are that the propagation medium is horizontally stratified and range independent, multiple scattering between the object and waveguide boundaries is negligible, the object lies within a constant sound speed layer, and the range from the object to the source or receiver is large enough that the scattered field can be expressed as a linear function of the object's plane wave scatter function.

Under these conditions, the plane wave scatter function of the object, which depends on absolute object orientation and direction of both the incident and scattered plane wave, is the invariant quantity that describes the scattering properties of an object in a waveguide. The scatter function is a coherent quantity. The object's incoherent target strength is simply 20 log of the scatter-function-magnitude-to-wave number ratio. Target strength then only contains the amplitude but not the essential phase information necessary to describe the scattering process in a waveguide.

We show analytically that if the scatter function of the object is approximately constant over the equivalent angles spanned by the waveguide modes for the given bistatic geometry, the scatter function of the object, which effectively couples the modes of the incident and scattered field, can be factored with little error. This leads to an approximation for the sound pressure level of the scattered field that is the sonar equation. Many rounded objects, such as spheres and certain spheroids, exhibit this behavior in nonforward scatter. Flat homogeneous objects, such as plates and disks, are the most highly directional convex targets. These have nonuniform scatter functions with strong main lobes in the forward and backscatter directions of diffraction-limited angular width λ/L, for $\lambda/L \ll 1$, where L is the object's length and λ the wavelength. Other targets that are nonconvex or inhomoge-

neous, for example, may have a narrower scatter function main lobe due to interference from distinct parts of the target. In the limit, the scatter function of an object consisting solely of two point scatterers separated by L has the narrowest main lobe of angular width $\lambda/2L$. When the angular width of the object's scatter function main lobe is much smaller than that spanned by the propagating modes $\pm \Delta \psi$ about the horizontal, which is often limited by the critical angle ψ_c of the seabed beyond a few water column depths in range, the modes of the waveguide are scattered nonuniformly. This leads to strong coupling between propagation and scattering in both the forward and backscatter azimuths. The sonar-equation approximation is found to be in error, often by tens of decibels, when applied to such highly directional targets in shallow water waveguides.

These findings explain the physical basis for the discrepancy noted in Ref. 9 between the sonar equation and a waveguide scattering model. Some special cases were previously noted. For example, Ingenito pointed out that propagation and scattering become factorable in a waveguide that supports only a single mode.[7] Makris noted that this factorization is possible for compact objects, i.e., those with $ka = \pi L/\lambda \ll 1$.[9] We note that the sonar equation is always valid for compact pressure-release objects since the scattered field is effectively omnidirectional, but is more approximate for rigid compact objects since their scattered fields always maintain some directionality as ka decreases.

As a general conclusion, we find that *the sonar equation is valid when the target's scatter function is roughly constant over the equivalent horizontal grazing angles $\pm \Delta \psi$ spanned by the dominant waveguide modes.* This is approximately true (1) for all objects when $2\Delta \psi < \lambda/2L$ and (2) for spheres and certain other rounded objects in nonforward scatter azimuths even when (1) does not hold. For homogeneous convex objects condition (1) is the less stringent $2\Delta \psi < \lambda/L$. A quantitative definition of $\Delta \psi$ is provided in Sec. III B. It should be noted that $\Delta \psi$ is range dependent in realistic ocean waveguides and is not necessarily equal to the critical angle ψ_c. This is true even in Pekeris waveguides at small ranges where the leaky modes with elevation angles larger than ψ_c make substantial contribution to the scattered field and at long ranges where modal stripping reduces the dominant modes to elevation angles much smaller than ψ_c.

This conclusion is significant because, in an active scenario, the sonar operator has the ability to lower the frequency of transmission until the target's scatter function becomes approximately constant over $\pm \Delta \psi$. The sonar equation then becomes a valid approximation when $f < c/(4L\Delta \psi)$. Operating in this frequency regime is desirable because when the sonar equation is valid, only a single parameter is necessary to characterize the scattering properties of the target for that measurement. This greatly simplifies target classification by making the classic approach of estimating a single-parameter target strength valid in a shallow water waveguide. It also simplifies other problems such as estimating target depth in a waveguide. When the sonar equation is not valid, the problem of classifying the target becomes much more complicated. Up to $2(2N)^2$ parameters would be necessary to characterize the scattering properties

of the target, for a waveguide that supports N modes, because the amplitude and phase of the object's scatter function would have to be determined for each incident and scattered pairing of each mode's equivalent up- and downgoing plane wave elevation angles.

Babinet's principle maintains that the forward scattered fields of impenetrable objects that have identical projected areas with respect to a given incident plane wave in free space are asymptotically equal for large ka.[10,12,13] This also holds true for some penetrable objects.[10] For an object submerged in a waveguide, the incident and scattered fields are often characterized by a wide angular spectrum of plane waves. Despite this difference between waveguide and free space scattering, simulations in several typical shallow water waveguides with a variety of targets types show that Babinet's principle can hold approximately in a waveguide *in the forward-scatter azimuth* if the equivalent propagation angles of the modes are sufficiently close to horizontal, as if often the case after long-range propagation in lossy media. By Babinet's principle, objects that are large compared to the wavelength cast the same free space shadow as flat objects with the same projected area. Since flat objects of high ka are the most directional, the sonar equation approximation breaks down rapidly in a shallow water waveguide as ka increases beyond unity for scattering in the *forward* azimuth for all object shapes, including spheres. Extreme caution should then be used in applying the sonar equation in forward scatter.

In Sec. II, we describe the waveguide scattering model that takes into account the coupling between propagation and scattering in a shallow water waveguide. A detailed derivation of the sonar equation from Green's Theorem is provided in Sec. III to show when propagation and scattering become decoupled and when incoherent target strength is sufficient to describe the scattering properties of an object in a waveguide. Illustrative examples are presented in Sec. IV. Babinet's principle and issues involved with applying it in a waveguide are discussed in Sec. V.

II. WAVE-THEORETIC MODEL FOR 3-D SCATTERING FROM AN OBJECT OF ARBITRARY SHAPE IN A STRATIFIED MEDIUM

We adopt a wave-theoretic normal mode model based on Green's Theorem for the field scattered by an object in a stratified medium, following Refs. 7 and 8. In the formulation, the origin of the coordinate system is placed at the object centroid. The source coordinates are defined by $r_0 = (x_0, y_0, z_0)$ and the receiver coordinates by $r = (x, y, z)$, where the positive z axis points downward and normal to the interface between horizontal strata. Spatial cylindrical (ρ, ϕ, z) and spherical systems (r, θ, ϕ) are defined by $x = r \sin \theta \cos \phi$, $y = r \sin \theta \sin \phi$, $z = r \cos \theta$, and $\rho = x^2 + y^2$. The horizontal grazing angle is $\psi = \pi/2 - \theta$. The horizontal and vertical wave number components for the nth mode are, respectively, $\xi_n = k \sin \alpha_n$ and $\gamma_n = k \cos \alpha_n$, where α_n is the elevation angle of the mode measured from the z axis. Here $0 \leq \alpha_n \leq \pi/2$ so that the down- and upgoing plane wave components of each mode will then have elevation angles α_n and $\pi - \alpha_n$, respectively. The corresponding ver-

tical wave number of the down and upgoing components of the nth mode are γ_n and $-\gamma_n$, respectively, where $\text{Re}\{\gamma_n\} \geq 0$. Moreover, $k^2 = \xi_n^2 + \gamma_n^2$, and the wave number magnitude k equals the angular frequency ω divided by the sound speed c in the object layer. For economy, the notation of Ref. 11 is used here and in the remainder of this article. Figure 2 of Ref. 11 shows the geometry of spatial and wave number coordinates.

The spectral component of the scattered field from the object at the origin for a source at r_0 and a receiver at r is

$$\Phi_s(r|r_0) = \mathcal{A} \sum_{m=1}^{M_{\max}} \sum_{n=1}^{M_{\max}} \frac{(4\pi)^2}{k}$$
$$\times [A_m(r)A_n(r_0)S(\pi - \alpha_m, \beta; \alpha_n, \beta_i)$$
$$- B_m(r)A_n(r_0)S(\alpha_m, \beta; \alpha_n, \beta_i)$$
$$- A_m(r)B_n(r_0)S(\pi - \alpha_m, \beta; \pi - \alpha_n, \beta_i)$$
$$+ B_m(r)B_n(r_0)S(\alpha_m, \beta; \pi - \alpha_n, \beta_i)], \quad (1)$$

where

$$A_m(r) = \frac{i}{d(0)} (8\pi \xi_m \rho)^{-1/2} u_m(z) N_m^{(1)} e^{i(\xi_m \rho + \gamma_m D - \pi/4)},$$

$$B_m(r) = \frac{i}{d(0)} (8\pi \xi_m \rho)^{-1/2} u_m(z) N_m^{(2)} e^{i(\xi_m \rho - \gamma_m D - \pi/4)},$$

$$A_n(r_0) = \frac{i}{d(z_0)} (8\pi \xi_n \rho_0)^{-1/2} u_n(z_0) N_n^{(1)} e^{i(\xi_n \rho_0 + \gamma_n D - \pi/4)},$$

$$B_n(r_0) = \frac{i}{d(z_0)} (8\pi \xi_n \rho_0)^{-1/2} u_n(z_0) N_n^{(2)} e^{i(\xi_n \rho_0 - \gamma_n D - \pi/4)},$$

(2)

are the incident and scattered down- and upgoing plane wave amplitudes in the layer of the object, $\mathcal{A}$ is the source amplitude, D is the depth of the object center from the sea surface, $d(z)$ is the density at depth z, $u_n(z)$ are the mode functions, $S(\alpha, \beta, \alpha_i, \beta_i)$ is the object's plane wave scatter function, and $M_{\max}$ is the mode number at which the series can be truncated and still accurately represent the field. The definition of the plane wave scatter function here follows that defined in Ref. 8, where the incident plane wave on the object is described in terms of the direction it goes to so that for forward scatter in free space $\alpha = \alpha_i$, $\beta = \beta_i$. The product of $e^{-i2\pi ft}$ and the right hand side of Eq. (1) yields the time-harmonic scattered field. The mode functions are normalized according to

$$\delta_{nm} = \int_{-D}^{\infty} \frac{u_m(z)u_n^*(z)}{d(z)} dz, \quad (3)$$

and can be expressed in the layer of the object as

$$u_n(z) = N_n^{(1)} e^{i\gamma_n(z+D)} - N_n^{(2)} e^{-i\gamma_n(z+D)}, \quad (4)$$

where $N_n^{(1)}$ and $N_n^{(2)}$ are normalization constants.

A more general expression than Eqs. (1)–(4), for the scattered field from an arbitrarily shaped object in a stratified medium, is given in Refs. 9 and 11 in terms of wave number integrals. A number of assumptions have to be satisfied for the above formulation to be valid, as noted in Ref. 8. In particular, multiple scattering between the object and wave-
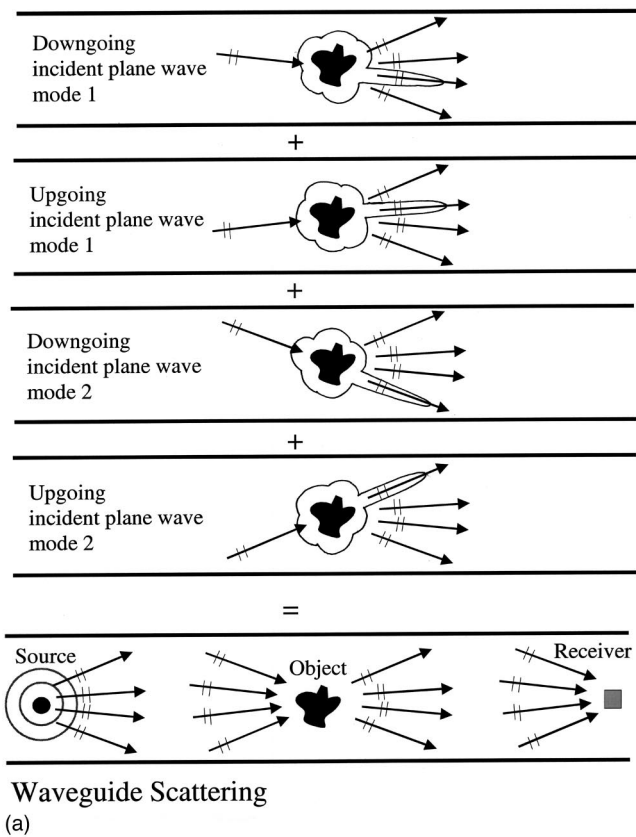
Waveguide Scattering

(a)
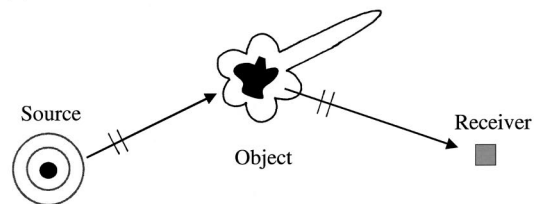
Free Space Scattering

(b)

FIG. 1. (a) Scattering in a waveguide with only two modes. Each mode is composed of a downgoing and an up-going plane wave. Each incoming plane wave is scattered by the object into various outgoing plane waves. The scattered fields from each incident plane wave are coherently superposed to form the total scattered field at the receiver. (b) Scattering in free space. Scattering by the object depends only on the direction of the source and receiver relative to the target in free space in the farfield.

guide boundaries is negligible, the object lies within a layer of constant sound speed, and the range from the object to source or receiver must be large enough that the scattered field can be approximated as a linear function of the object's plane wave scatter function and by modal summations.

In Eq. (1), the field radiated by the source is decomposed into modes incident on the object. Each incoming mode is composed of a pair of plane waves: one downgoing with amplitude $A_n(\mathbf{r}_0)$ and one up-going with amplitude $B_n(\mathbf{r}_0)$ with incident elevation angles, α_n and $\pi - \alpha_n$, respectively. Each scattered mode is also composed of a pair of plane waves with amplitude $B_m(\mathbf{r})$ and elevation angle α_m for the downgoing plane wave and amplitude $A_m(\mathbf{r})$ and elevation angle $\pi - \alpha_m$ for the upgoing plane wave.[15] Each of the four terms in Eq. (1) represents the *coherent* scattering of one of the two incoming plane wave components of the nth

mode, into one of the two outgoing plane wave components of the mth mode. The farfield physics of the interaction is determined by the scatter function that depends on the elevation angles of both the incident and scattered plane waves. The scatter function is a coherent quantity that affects both the amplitude and phase of the scattered plane waves. The scattered fields from each incident plane wave are coherently superposed to form the total scattered field at the receiver. The scattering process couples the modes so that propagation and scattering are coherently convolved for objects submerged in a shallow water waveguide. A conceptual diagram of scattering in a waveguide is given in Fig. 1(a) for a waveguide that excites only two modes.

We would like to point out some errata in Ref. 8. In Eqs. (14)–(17) and (37) of Ref. 8, the functions B_m and $B_{m'}^*$ should be replaced by A_m and $A_{m'}^*$, respectively, in Eqs. (41) and (43)–(45), the functions B_l and B_l^* should be replaced by A_l and A_l^* respectively, and in Eqs. (14) and (15), the angles α_m and $\alpha_{m'}$ should be replaced with $\pi - \alpha_m$ and $\pi - \alpha_{m'}$ respectively. In Eqs. (42)–(45), the vertical wavenumber γ_l should be replaced with $-\gamma_l$ and the vertical wavenumber $-\gamma_m$ should be replaced by $+\gamma_m$.[15]

III. THE SONAR EQUATION

A. Sonar equation model for the scattered field from an object in free space

Here we derive the sonar equation from first principles using Green's theorem and some steps from Appendix A of Ref. 8. With the object centroid at the origin of the coordinate system, let the coordinates of a point on the surface of the object be defined by $\mathbf{r}_t = (x_t, y_t, z_t)$. Using the Helmholtz–Kirchoff integral equation,[12] the harmonic field scattered by an object can be expressed as

$$\Phi_s(\mathbf{r}) = -\oiint_{A_t} \left\{ [\Phi_i(\mathbf{r}_t) + \Phi_s(\mathbf{r}_t)] \frac{\partial G(\mathbf{r}|\mathbf{r}_t)}{\partial n_t} - G(\mathbf{r}|\mathbf{r}_t) \frac{\partial}{\partial n_t} [\Phi_i(\mathbf{r}_t) + \Phi_s(\mathbf{r}_t)] \right\} dA_t, \quad (5)$$

where $G(\mathbf{r}|\mathbf{r}_t)$ is the medium's Green's function and $\Phi_i(\mathbf{r}_t)$ is the incident field, each satisfying the Helmholtz equation driven by a source at angular frequency $\omega = 2\pi f$. The area integral encloses the scatterer and the surface normal points into the enclosed volume.

In free space, for a point source at location $\mathbf{r}_0$, the field incident on the object is approximately planar for $r_0 \gg r_t$ and can be expressed as

$$\Phi_i(\mathbf{r}_t) = \mathcal{A} \frac{e^{ik|\mathbf{r}_t - \mathbf{r}_0|}}{|\mathbf{r}_t - \mathbf{r}_0|} \approx \mathcal{A} \frac{e^{ikr_0}}{r_0} e^{ikr_t \eta(\alpha_i, \beta_i, \theta_t, \phi_t)}, \quad (6)$$

where (α_i, β_i) is the direction the plane wave from the source travels to, and the cosine between the directions (θ_t, ϕ_t) and (α_i, β_i) is

$$\eta(\alpha_i, \beta_i, \theta_t, \phi_t) = \cos \alpha_i \cos \theta_t + \sin \alpha_i \sin \theta_t \cos (\beta_i - \phi_t). \quad (7)$$

The Green's function in free space is

Ratital *et al.*: Sonar equation and Babinet's principle in a stratified medium

$$G(\mathbf{r}|\mathbf{r}_t) = \frac{1}{4\pi} \frac{e^{ik|\mathbf{r}-\mathbf{r}_t|}}{|\mathbf{r}-\mathbf{r}_t|} \approx \frac{1}{4\pi} \frac{e^{ikr}}{r} e^{-ikr_t \eta(\alpha,\beta,\theta_t,\phi_t)}, \quad (8)$$

where the last approximation is for a receiver so far from the object that $r \gg r_t$. By application of Green's theorem, the scattered field at this distant receiver then can be written as

$$\Phi_s(\mathbf{r}) = -\mathcal{A} \frac{e^{ikr_0}}{r_0} \frac{e^{ikr}}{4\pi r} \oiint_{A_t} \left\{ \left(e^{ikr_t \eta(\alpha_i,\beta_i,\theta_t,\phi_t)} + \frac{r_0}{\mathcal{A}} e^{-ikr_0} \Phi_s(\mathbf{r}_t) \right) \frac{\partial}{\partial n_t} e^{-ikr_t \eta(\alpha,\beta,\theta_t,\phi_t)} \right.$$
$$\left. - e^{-ikr_t \eta(\alpha,\beta,\theta_t,\phi_t)} \frac{\partial}{\partial n_t} \left(e^{ikr_t \eta(\alpha_i,\beta_i,\theta_t,\phi_t)} + \frac{r_0}{\mathcal{A}} e^{-ikr_0} \Phi_s(\mathbf{r}_t) \right) \right\} dA_t. \tag{9}$$

By definition of the plane wave scatter function $S(\alpha,\beta,\alpha_i,\beta_i)$, however, Eq. (9) can also be written as

$$\Phi_s(\mathbf{r}) = \mathcal{A} \frac{e^{ikr_0}}{r_0} \frac{e^{ikr}}{kr} S(\alpha,\beta,\alpha_i,\beta_i), \tag{10}$$

in an object-centered coordinate system, which leads to the equality

$$S(\alpha,\beta,\alpha_i,\beta_i) = -\frac{k}{4\pi} \oiint_{A_t} \left\{ \left(e^{ikr_t \eta(\alpha_i,\beta_i,\theta_t,\phi_t)} + \frac{r_0}{\mathcal{A}} e^{-ikr_0} \Phi_s(\mathbf{r}_t) \right) \frac{\partial}{\partial n_t} e^{-ikr_t \eta(\alpha,\beta,\theta_t,\phi_t)} \right.$$
$$\left. - e^{-ikr_t \eta(\alpha,\beta,\theta_t,\phi_t)} \frac{\partial}{\partial n_t} \left(e^{ikr_t \eta(\alpha_i,\beta_i,\theta_t,\phi_t)} + \frac{r_0}{\mathcal{A}} e^{-ikr_0} \Phi_s(\mathbf{r}_t) \right) \right\} dA_t, \tag{11}$$

that relates Eq. (9) directly to the Green's theorem when $r \gg r_t$.

Using the free space Green's function, Eq. (8), we can write Eq. (10) as

$$\Phi_s(\mathbf{r}) = \mathcal{A}(4\pi)^2 G(\mathbf{0}|\mathbf{r_0}) G(\mathbf{r}|\mathbf{0}) \frac{S(\alpha,\beta,\alpha_i,\beta_i)}{k}. \tag{12}$$

From Eq. (12), we see that the Green's functions that describe the propagation of waves from source to object $G(\mathbf{0}|\mathbf{r_0})$ and from object to receiver $G(\mathbf{r}|\mathbf{0})$ are decoupled from the scattering function $S(\alpha,\beta,\alpha_i,\beta_i)$ of the object that governs the scattering process. Only the directions of the source and the receiver relative to the object matter for farfield scattering in free space where propagation and scattering effects become factorable from each other. The approximation given in Eq. (12) is always valid in the farfield, where $r, r_0 > L^2/\lambda$, and may be valid at much closer ranges for certain targets, such as spheres.[9] The incident wave effectively arrives at the target as a plane wave propagating from the direction of the source and the scattered wave at the point receiver behaves as a plane wave propagating from the target centroid. The scatter function of the target determines how a plane wave from the source is scattered in the direction of the receiver.

It is important to notice that Eq. (12) is in the frequency domain for a time harmonic source. If the source was broadband with spectrum $Q(f)$, the received field would be the inverse Fourier transform of the product of $Q(f)$ and the right-hand side of Eq. (12). For a broadband source signal, it is impossible to separate scattering from propagation even in free space. For a narrow band source, $\mathcal{A} \approx Q(f)df$.

Equation (10) can be recast as a sonar equation by taking 10 log of the squared magnitude of both sides,

$$10\log\left(\frac{|\Phi_s(\mathbf{r})|^2}{P_{\text{ref}}^2} \right) = \text{SL} - \text{TL}(\mathbf{0}|\mathbf{r_0}) + \text{TS} - \text{TL}(\mathbf{r}|\mathbf{0}), \tag{13}$$

where $P_{\text{ref}} = 1$ μPa, $r_{\text{ref}} = 1$ m, and

$$\text{SL} = 20\log\left| \frac{\mathcal{A}}{P_{\text{ref}} r_{\text{ref}}} \right| \quad \text{dB } re \text{ 1 } \mu\text{Pa at 1 m}, \tag{14}$$

$$\text{TL}(\mathbf{0}|\mathbf{r_0}) = 20\log\frac{r_0}{r_{\text{ref}}} \quad \text{dB } re \text{ 1 m}, \tag{15}$$

$$\text{TS} = 20\log\left| \frac{S(\alpha,\beta,\alpha_i,\beta_i)}{k r_{\text{ref}}} \right| \quad \text{dB } re \text{ 1 m}, \tag{16}$$

$$\text{TL}(\mathbf{0}|\mathbf{r}) = 20\log\frac{r}{r_{\text{ref}}} \quad \text{dB } re \text{ 1 m}. \tag{17}$$

Following the sonar equation, the radiated sound has a source level of SL, which is the sound pressure level measured at 1 m from the source. This is reduced by the transmission loss $\text{TL}(\mathbf{r_0}|\mathbf{0})$, from source to target centroid. The level is augmented by the target strength TS, and further diminished by transmission loss $\text{TL}(\mathbf{0}|\mathbf{r})$ from target centroid to receiver. The level of the scattered field in decibels, Eq. (13), is a linear combination of these incoherent quantities. The incoherent target strength is obtained from the magnitude of the free space scatter function following Eq. (16). It contains only the amplitude but not the phase information of the coherent scatter function and depends only on the direc-

B. Application of the sonar equation in a waveguide

It is common practice when using the sonar equation in a waveguide to replace the transmission loss in free space with that in the waveguide.[2] This can be done analytically by replacing the free-space Green's function with the waveguide Green's function in Eq. (12). Using a modal formulation, the Green's function in the waveguide between a point at the origin $\mathbf{0}$ and a field point at r can be expressed as a sum of normal modes,

$$G(\mathbf{r}|\mathbf{0}) = \frac{i}{d(0)}(8\pi)^{-1/2}e^{-i\pi/4}\sum_{m}^{M_{\max}} u_m(z)u_m(0)\frac{e^{i\xi_m\rho}}{\sqrt{\xi_m\rho}}. \tag{18}$$

Using Eqs. (2) and (4), we can express the Green's function in the waveguide, Eq. (18), as

$$G(\mathbf{r}|\mathbf{0}) = \sum_{m}^{M_{\max}} [A_m(\mathbf{r}) - B_m(\mathbf{r})]. \tag{19}$$

By reciprocity,

$$G(\mathbf{0}|\mathbf{r}_0) = G(\mathbf{r}_0|\mathbf{0}) = \sum_{n}^{M_{\max}} [A_n(\mathbf{r}_0) - B_n(\mathbf{r}_0)]. \tag{20}$$

Substituting the waveguide Green's functions, Eqs. (19) and (20) into Eq. (12), we obtain the sonar equation approximation for the scattered field from an object in a waveguide:

$$\Phi_s(\mathbf{r}|\mathbf{r}_0) = \mathcal{A}(4\pi)^2 \left(\sum_{n}^{M_{\max}} [A_n(\mathbf{r}_0) - B_n(\mathbf{r}_0)] \right)$$
$$\times \left(\sum_{m}^{M_{\max}} [A_m(\mathbf{r}) - B_m(\mathbf{r})] \right) \frac{S(\alpha,\beta,\alpha_i,\beta_i)}{k}. \tag{21}$$

The wave-theoretic model for object scattering in a waveguide, Eq. (1), differs significantly from the sonar equation model in Eq. (21). In the waveguide scattering model, the scattered field depends on the direction of each incoming and outgoing modal plane wave. Each incoming plane wave is *coherently* scattered to each outgoing plane wave by the object depending on the scatter function, which can vary with the azimuth and elevation angles of the incoming and outgoing plane waves. In the sonar equation model, since propagation and scattering are assumed to decouple, the scattered field depends only on the direction of the source and receiver relative to the object and not the direction of the individual modal plane waves.

The sonar equation (21) is a special case of the general coherent scattering formulation for a waveguide of Eq. (1), and so is only valid under restrictive conditions. If the scatter function remains constant over the horizontal grazing angle span of the waveguide modes $\pm\Delta\psi$ for the given measurement scenario, the scatter function factors from the modal sums of the waveguide scattering model, Eq. (1), that then reduces to the sonar equation, Eq. (21). Propagation and

scattering are then separable, and the sonar equation becomes valid in a waveguide where α and α_i are approximately $\pi/2$ in Eq. (21). Target strength, along with the other incoherent terms of the sonar equation, SL and TL, then become sufficient to determine the scattered field level in decibels. We approximate the horizontal grazing angle span of the waveguide modes by

$$\pm\Delta\psi = \pm\left(\frac{\pi}{2} - \alpha_{M_{\max}}\right), \tag{22}$$

where

$$\alpha_{M_{\max}} = \tan^{-1}\frac{\xi_{M_{\max}}}{\gamma_{M_{\max}}}. \tag{23}$$

Here $M_{\max}$ and $\Delta\psi$ are range-dependent, even in realistic range-independent waveguides, and tend to decrease with range due to attenuation from absorption and scattering in the ocean, following the process known as ''mode stripping.'' This is significant because the sonar equation approximation improves as $\Delta\psi$ decreases for fixed λ/L.

IV. ILLUSTRATIVE EXAMPLES IN SHALLOW WATER

We now use examples to illustrate the fact that the sonar equation is valid when the scatter function is roughly constant over the equivalent horizontal grazing angles spanned by the dominant waveguide modes. We show that the sonar equation is generally a good approximation (1) for all objects when $2\Delta\psi < \lambda/2L$, for homogeneous convex objects when $2\Delta\psi < \lambda/L$, and (2) for spheres and certain other rounded objects in nonforward scatter azimuths, even when (1) does not hold. We proceed by analyzing active sonar examples for a variety of target types and shallow water waveguides with both the sonar equation and the waveguide scattering model.

In all the illustrative examples, a water column of 100 m depth is used to simulate a typical continental shelf environment. The sound speed in the water column is isovelocity at 1500 m/s with a constant density of 1 g/cm^3 and attenuation of 6.0×10^{-5} dB/λ. The seabed is either perfectly reflecting or comprised of sand or silt half-spaces. The density, sound speed, and attenuation are taken to be 1.9 g/cm^3, 1700 m/s, and 0.8 dB/λ for sand, 1.4 g/cm^3, 1520 m/s, and 0.3 dB/λ for silt. The receiver is either colocated with the source, in which case we calculate the backscattered field where $\beta_i = 0$, $\beta = \pi$, or in the forward azimuth of the object where $\beta_i = \beta = 0$ and we calculate the forward scattered field. The scattered fields from a disk, sphere, spheroid, and composite target are computed as a function of increasing range between source–receiver and object. In all the examples, the range increases along the x axis and depth along the z axis.

A. Effect of bottom type on the validity of the sonar equation

We use examples to illustrate how the validity of the sonar equation depends on the bottom type through the grazing angle span of the waveguide modes $\Delta\psi$. In a Pekeris
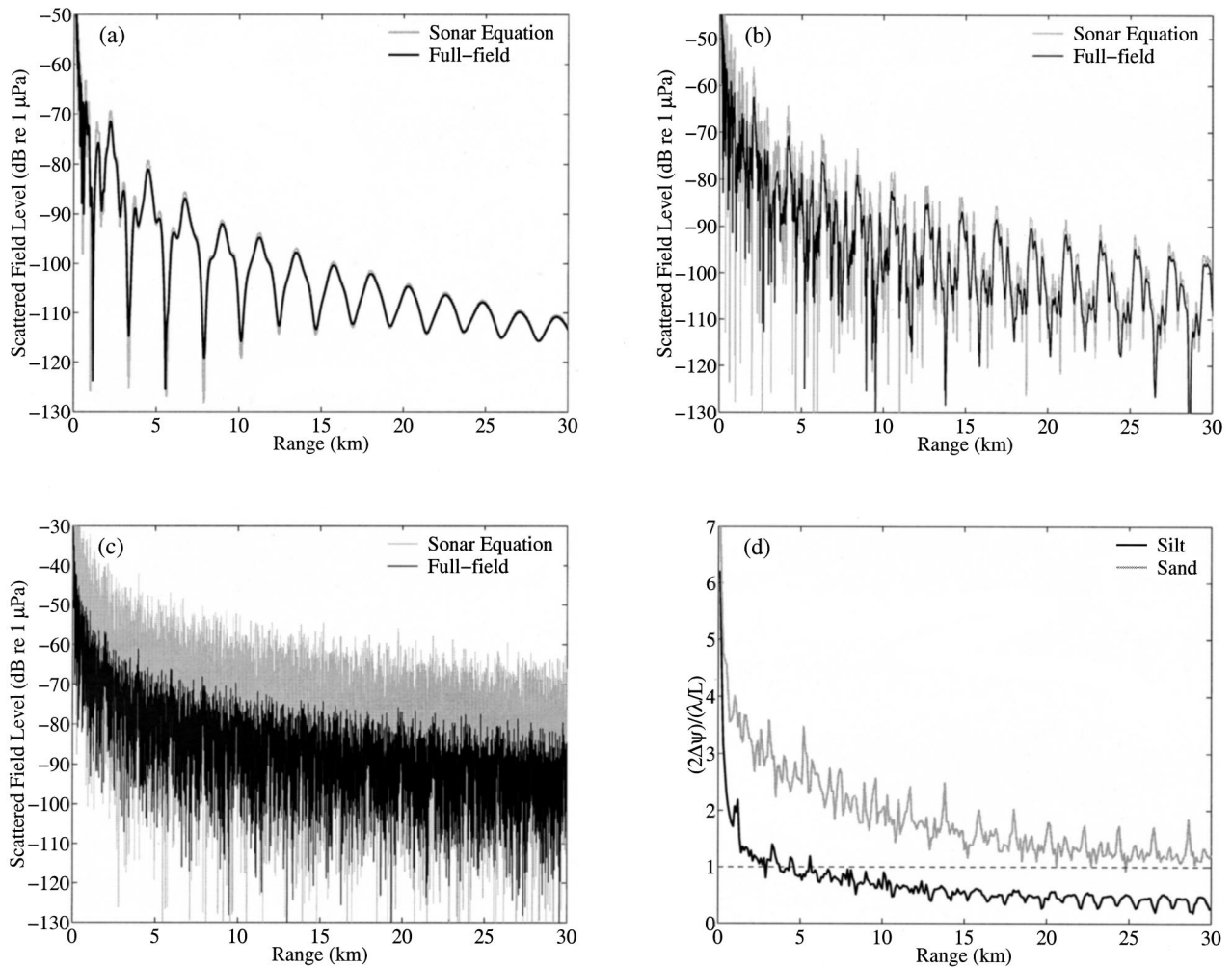
FIG. 2. The backscattered field from an upright 10 m radius rigid circular disk at 300 Hz in Pekeris waveguides with (a) silt, (b) sand, and (c) perfectly reflecting bottoms, respectively, calculated using the waveguide scattering model, Eq. (1), and compared to the sonar equation, Eq. (21). The water depth is 100 m with the source–receiver and object at 50 m depth in the middle of the water column. The range increases along the x axis and depth along the z axis. The circular disk is aligned with its plane normal to the x axis. The results are plotted in decibels, i.e., $20 \log|\Phi_s|$, as a function of increasing range between the object and monostatic source–receiver. The source level is 0 dB re 1 μPa at 1 m. ka is 12.6 for this example. (d) The ratio $2\Delta\psi/(\lambda/L)$ for the examples given in (a) and (b). For the perfectly reflecting waveguide $2\Delta\psi/(\lambda/L)$ is 12.6. The sonar equation provides a good approximation to the scattered field in the waveguide when $2\Delta\psi/(\lambda/L)<1$.

waveguide, $\Delta\psi$ is bounded by the critical grazing angle of the bottom ψ_c beyond a few waveguide depths in range where the leaky modes no longer contribute significantly. A bottom with a large sound speed contrast relative to the water column has a correspondingly large ψ_c, $M_{\max}$ and $\Delta\psi$. So for fixed source frequency and object size, the sonar equation approximation is expected to improve as this sound speed contrast decreases. We show this by examining Pekeris waveguides with silt, sand, and perfectly reflecting bottoms that, respectively, exhibit an increase in sound speed contrast.

The backscattered field from a homogeneous convex object, an upright 10 m radius rigid circular disk at 300 Hz, is plotted in Figs. 2(a)–(c) for the three bottom types. For this example, the product $ka=\pi L/\lambda$ is 12.6, where a is the radius of the disk, and ka is the ratio of the object circumference to the wavelength. By applying Green's theorem, the scatter function for the rigid circular disk is found to be
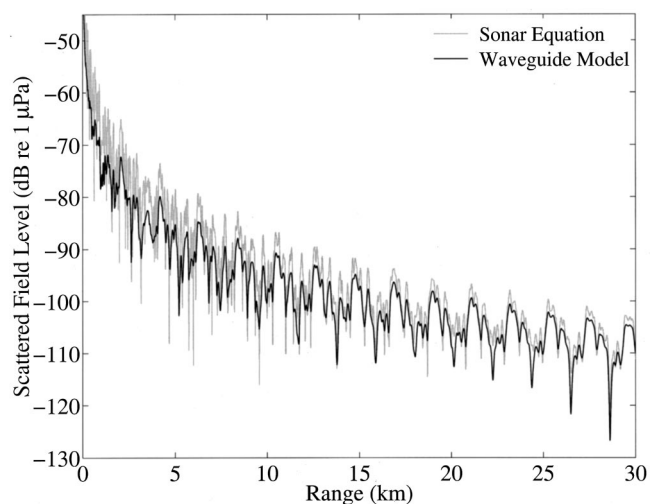

FIG. 3. Similar to Fig. 2(b), except the scattered field in the back azimuth is averaged over depth throughout the water column from 0 to 100 m.
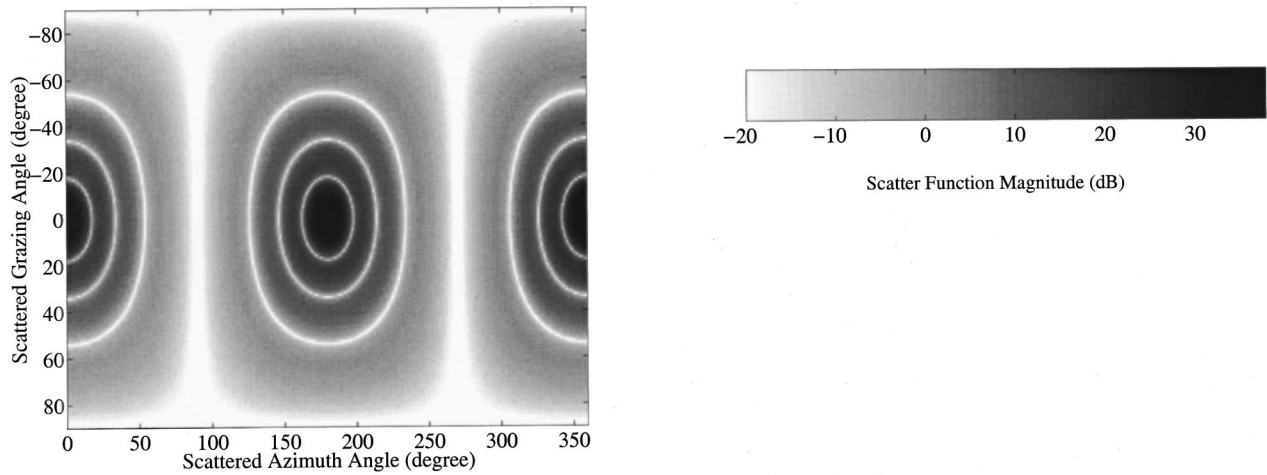
FIG. 4. The magnitude of the plane wave scatter function $20 \log |S(\alpha, \beta, \alpha_i = 90°, \beta_i = 0°)|$ for an upright rigid circular disk of $ka = 12.6$ is plotted as a function of horizontal grazing $(90° - \alpha)$ and azimuth β angles of scattered plane waves for an incident plane wave traveling in the direction $(90° - \alpha_i) = 0°, \beta_i = 0°$. The scatter function is antisymmetric about the plane of the disk, as can be seen from Eq. (24).

$$S(\alpha, \beta, \alpha_i, \beta_i) = -\frac{i}{2} \left(\frac{kL}{2} \right)^2 \sin \alpha \cos \beta \, \mathrm{circ}\left(\frac{kL}{2} \sqrt{(\sin \alpha_i \sin \beta_i - \sin \alpha \sin \beta)^2 + (\cos \alpha_i - \cos \alpha)^2} \right), \quad (24)$$

where $L = 2a$ is the diameter of the disk and $\mathrm{circ}(x) = 2J_1(x)/x$. An alternative but equivalent derivation and form for the scatter function can be found in Ref. 14.

As expected, the sonar equation matches the waveguide scattering model well in the Pekeris silt waveguide of Fig. 2(a) beyond roughly 5 km range. In the Pekeris sand waveguide, Fig. 2(b), the difference between the sonar equation and the waveguide scattering model is as much as 10 dB within a few kilometers range. The match, however, improves as the range increases. In the perfectly reflecting waveguide, Fig. 2(c), the sonar equation overestimates the scattered field level by as much as 20 dB. This error is more than half the object's maximum target strength of 36 dB re 1 m, which occurs monostatically at broadside. The scattered field shows greater fluctuation with range for the sonar equation approximation than for the waveguide scattering model. This is true in all three waveguides.

In practice, measurements are often averaged over space, time, or frequency to reduce the fluctuations that arise from waveguide interference. Less fluctuation with range is observed in both of the depth-averaged scattered fields of Fig. 3 than in Fig. 2(b) for the sand bottom. The discrepancy between the sonar equation and waveguide scattering model remains, however, with differences as large as 10 dB still occurring within a few kilometers range.

The reason that the sonar equation is found to be a good approximation for the silt beyond roughly 5 km but not the sand or perfectly reflecting waveguides is that the condition $2 \Delta \psi < \lambda / L$ only holds for the silt waveguide. This can be seen by examining Fig. 2(d), where the ratio $2 \Delta \psi / (\lambda / L)$ is plotted. Here $\Delta \psi$ is computed from Eqs. (22) and (23) at a given receiver depth by determining the minimum value for $M_{\max}$ at which the modal sum of Eq. (1) differs less than 1 dB from that of an infinite sum. The $\Delta \psi$ used in the figures is the average value over the receiver depth throughout the water column. For ranges beyond roughly 5 km in the silt waveguide, the ratio is less than unity and the condition for the sonar equation to be valid holds. Figure 2(d) also shows that the condition is generally not satisfied in the sand waveguide for the ranges shown. The condition is never satisfied in the
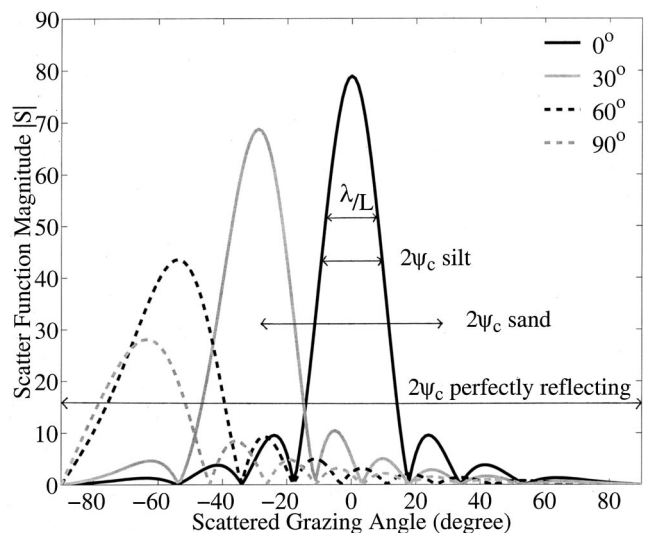

FIG. 5. The magnitude of the plane wave scatter function $|S(\alpha, \beta, \alpha_i, \beta_i = 0°)|$ for an upright rigid circular disk of $ka = 12.6$ is plotted as a function of the horizontal grazing angle $(90° - \alpha)$ of scattered plane waves in the backscatter azimuth $\beta = 180°$ for several incident plane waves with horizontal grazing angles $(90° - \alpha_i) = 0°, 30°, 60°,$ and $90°$. The solid curve in this figure for broadside incidence $[(90° - \alpha_i) = 0°]$ is a slice through Fig. 4 at the backscatter azimuth $\beta = 180°$ of the scattered plane waves. The width λ / L of the scatter function main lobe for broadside incidence is 14.3° or 0.25 rad. Also shown is the critical grazing angle ψ_c of the seabed in the Pekeris slit waveguide of 9.3°, Pekeris sand waveguide of 28°, and the perfectly reflecting waveguide of 90°.

perfectly reflecting waveguide because the ratio $2\Delta\psi/(\lambda/L)$ is always 12.6. As expected, the performance of the sonar equation improves with range in realistic ocean waveguides because M_{max} and $\Delta\psi$ decrease due to modal stripping, as is evident in Figs. 2(a), (b), and (d). Note that $\Delta\psi$ can be determined from Fig. 2(d) since $\lambda/L = 0.25$ rad or 14.3°, as can be seen from Figs. 4 and 5. Here the scatter function magnitude is plotted for the upright disk, where the main lobe has a minimum width of λ/L for a plane wave incident at broadside, where $(\pi/2 - \alpha_i) = 0$.

To visualize why the sonar equation is not valid when the condition $2\Delta\psi < (\lambda/L)$ does not hold, it is instructive to plot the width of the bottom critical angle for each bottom type across the scatter function main lobe, as is done in Fig. 5. When the condition does not hold, the object scatters the dominant incident modes with widely varying amplitudes and the scatter function cannot be approximated as a constant over $\pm\Delta\psi$. In this case, both the magnitude and phase variations of the scatter function are important in describing the scattering process. The sonar equation *overestimates* the level of the scattered field because it depends only on two

directions: those of the source and receiver relative to the object. The two relevant directions for the upright disk are $(\pi/2 - \alpha_i) = 0$ and $\beta_i = 0$ for the incident and $(\pi/2 - \alpha) = 0$ and $\beta = \pi$ for the scattered field. These correspond to global maxima in both the scatter function and target strength, as can be seen in Fig. 5, which is inappropriately assigned to all incoming and outgoing directions by the sonar equation.

B. Effect of object size and frequency on the validity of the sonar equation

In this section, we investigate sonar equation performance as a function of object size and frequency for a rigid circular disk in various waveguides. At the high ka of 62.8 shown in Figs. 6(a), (c), and (e), the object is large compared to the wavelength and the sonar equation significantly overestimates the scattered field level. This is to be expected from Fig. 6(g), where the condition $2\Delta\psi < \lambda/L$ is not satisfied in any of the waveguides. At the lower ka of 1.3, Figs. 6(b), (d), and (f), the sonar equation provides a good approximation in all except the perfectly reflecting waveguide,
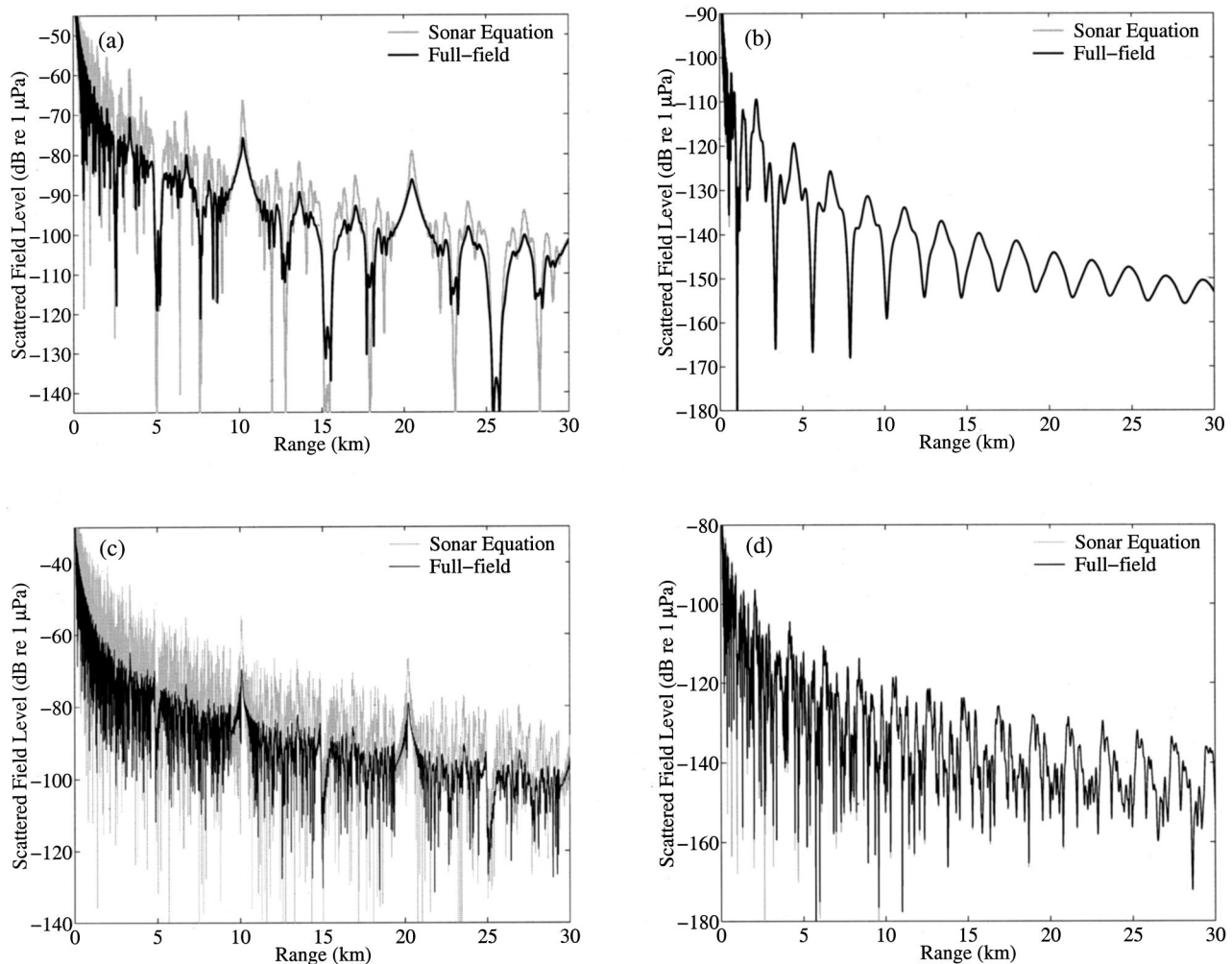

FIG. 6. Similar to Figs. 2(a)–(c), but for an upright rigid circular disk of (a) high and (b) low ka in the Pekeris silt waveguide, (c) high and (d) low ka in the Pekeris sand waveguide, and (e) high and (f) low ka in the perfectly reflecting waveguide. The high ka case corresponds to a disk of 10 m radius at 1500 Hz with $ka = 62.8$ while the low ka case corresponds to a disk of 1 m radius at 300 Hz with $ka = 1.3$. (g) and (h) are similar to Fig. 2(d) but for ka of 62.8 and 1.3, respectively for the cases shown in (a)–(d) in the Pekeris silt and sand waveguides. The ratio $2\Delta\psi/(\lambda/L) = 62.8$ for (e) with ka of 62.8 and $2\Delta\psi/(\lambda/L) = 1.3$ for (f) with ka of 1.3 in the perfectly reflecting waveguide.
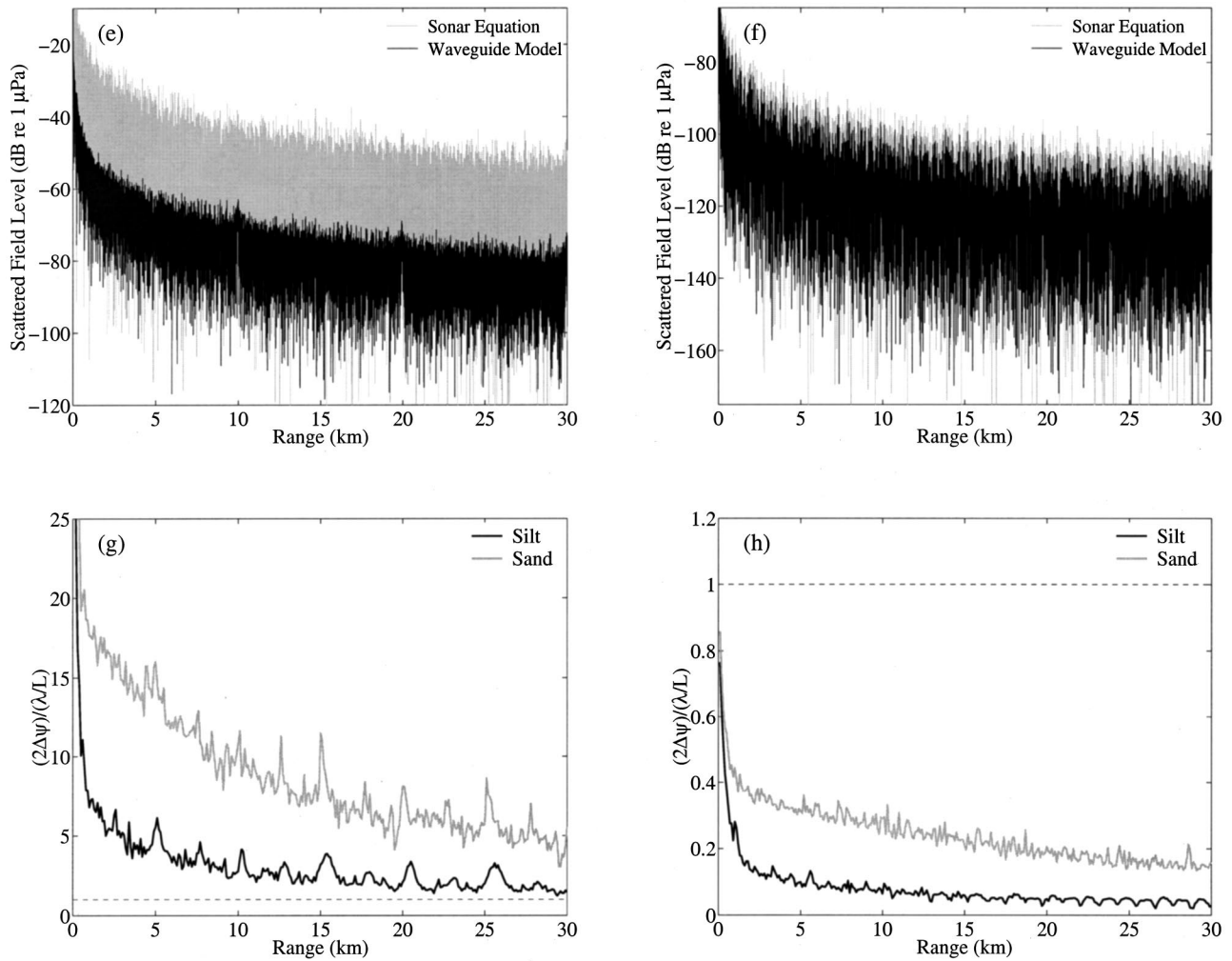
FIG. 6. (*Continued.*)

which is consistent with the results of Fig. 6(h), where the condition is satisfied for the sand and silt waveguides for all ranges shown. This shows that the sonar equation can be made valid for a given object and measurement geometry by lowering the frequency of operation. The scatter functions for the high and low *ka* cases are plotted in Figs. 7(a) and (b), respectively. For the low *ka* case in the perfectly reflecting waveguide, the width of the scatter function lobe is only
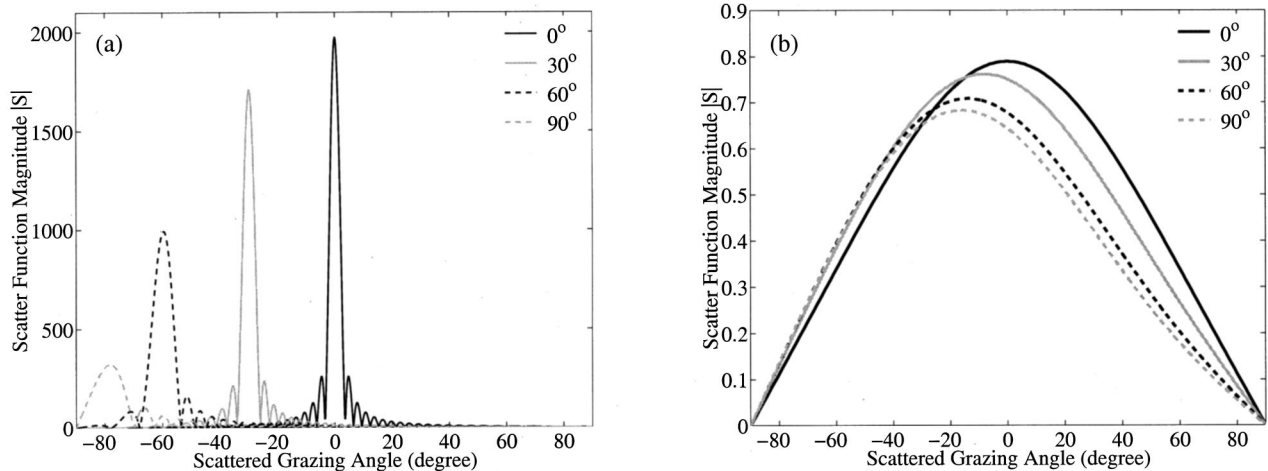

FIG. 7. Similar to Fig. 5, but for an upright rigid circular disk of (a) $ka = 62.8$ and (b) $ka = 1.3$. The width λ/L of the scatter function main lobe for broadside incidence $[(90° - \alpha_i) = 0°]$ is 2.9° or 0.05 rad for $ka = 62.8$ and 143° or 2.5 rad for $ka = 1.3$.
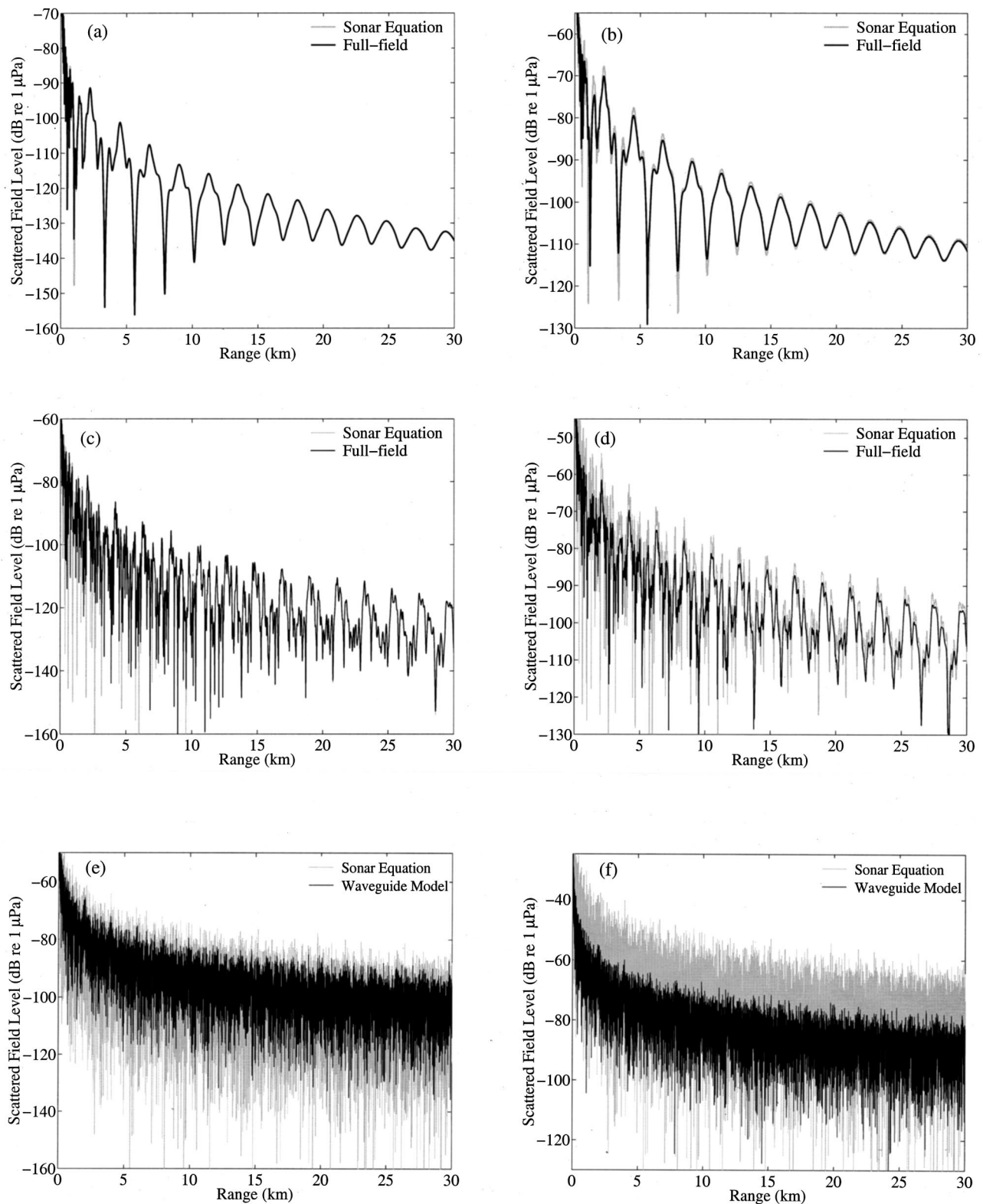
FIG. 8. Similar to Figs. 2(a)–(c) but for a 10 m radius pressure-release sphere at 300 Hz in the (a) back and (b) forward azimuths in Pekeris silt waveguide, the (c) back and (d) forward azimuths in Pekeris sand waveguide, and the (e) back and (f) forward azimuths in the perfectly reflecting waveguide. ka is 12.6 for this example.

slightly smaller than the full grazing angle span of the waveguide modes so the sonar equation provides only an order-of-magnitude approximation in backscatter.

In general, for pressure-release objects that are compact, small compared to the wavelength ($ka \ll 1$), the sonar equa-

tion approximation is always valid since the scattered field is effectively omnidirectional. For rigid objects that are compact, the sonar equation is still a good approximation, even though their scattered field always maintains some directionality as ka decreases.
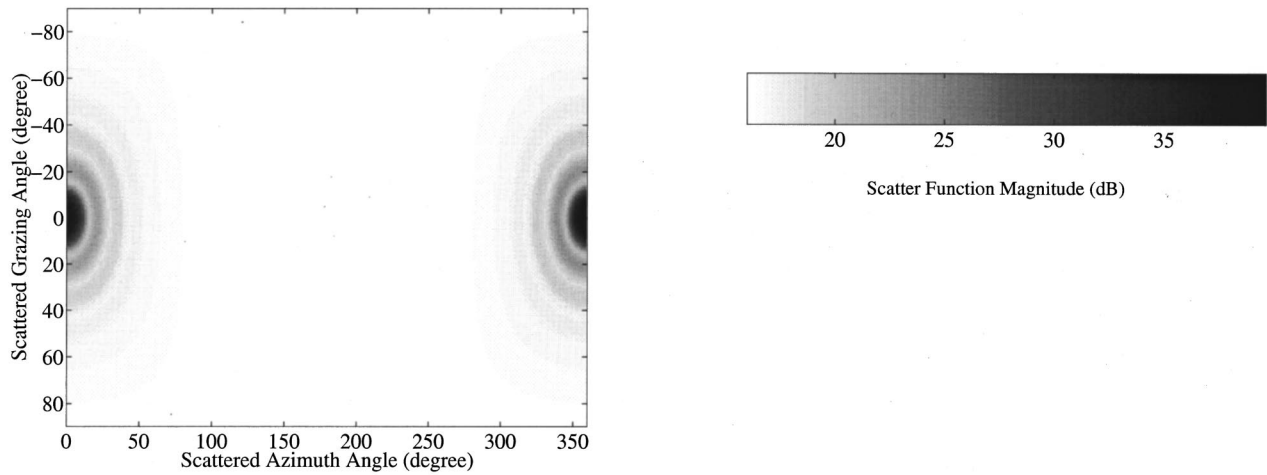
FIG. 9. Similar to Fig. 4, but for a pressure-release sphere of $ka = 12.6$. The scatter function for the sphere is given by Eqs. (8) and (9) of Ref. 9 with $f(n)$ replaced by $(-1)^n f(n)$ to convert from Ingenito's definition to the standard one described in Ref. 8. It can also be obtained from Ref. 14.
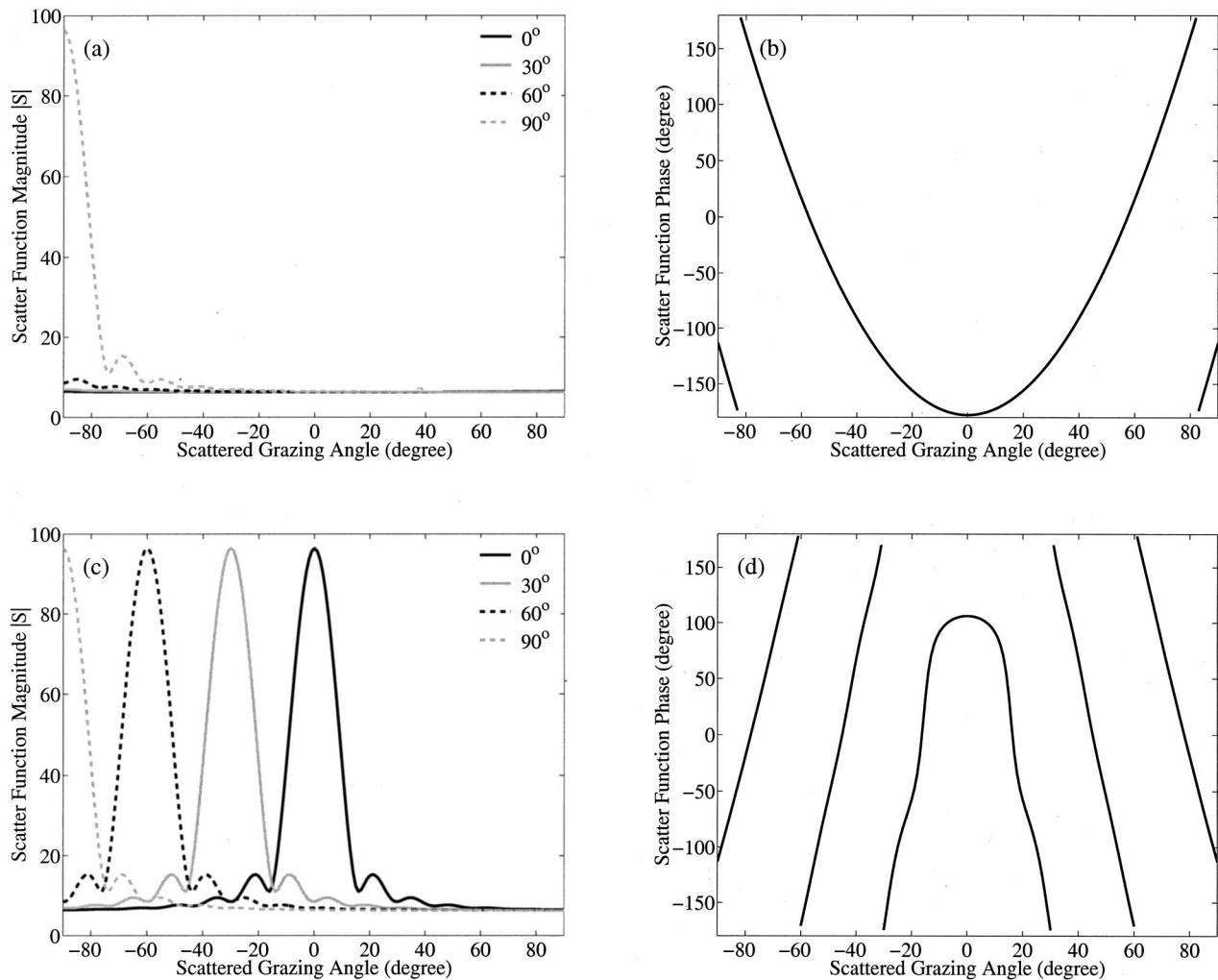

FIG. 10. (a) and (c) are similar to Fig. 5, but for a pressure-release sphere of $ka = 12.6$ plotted in the back ($\beta = 180°$) and forward ($\beta = 0°$) azimuths, respectively, of the scattered plane waves. The solid curves in (a) and (c) for $(90° - \alpha_i) = 0°$ are slices through Fig. 9 in the back and forward scatter azimuths, respectively. The width λ/L of the scatter function main lobe is $14.3°$ or 0.25 rad in (c). The phase of the scatter function for the solid curve [horizontal incidence, $(\alpha_i - 90°) = 0°$] in (a) and (c) is shown in (b) and (d), respectively, which are in the back and forward scatter azimuths.
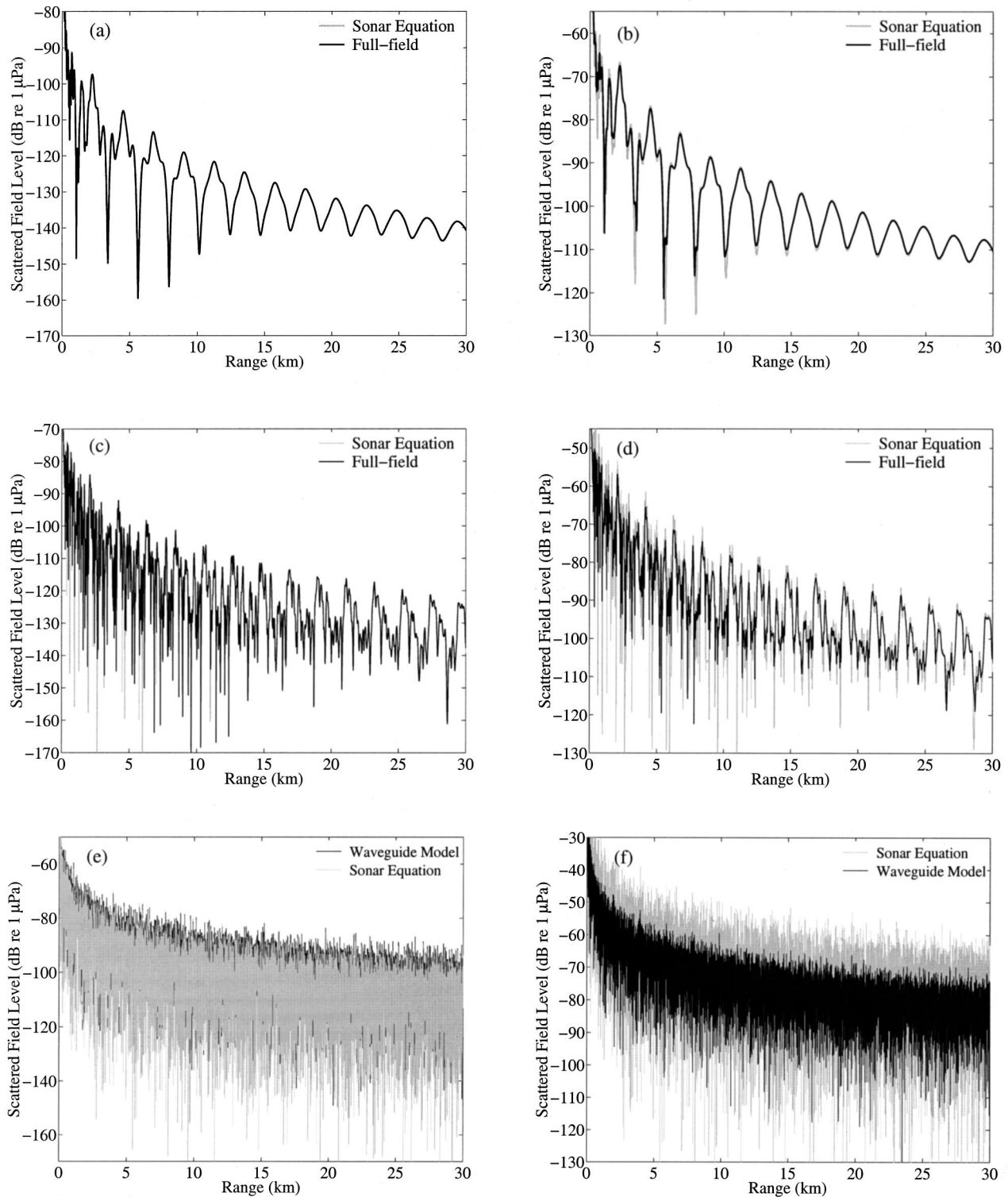
FIG. 11. Similar to Fig. 8, but for a pressure-release prolate spheroid of aspect ratio 2 with a major axis of 40 m and a minor axis of 20 m at 300 Hz. The spheroid is aligned such that the incoming plane waves are incident at the bow aspect where $ka = 12.6$.

C. Effect of orientation and shape of homogeneous convex targets on the validity of the sonar equation

In this section, we investigate the effect of orientation and shape on the validity of the sonar equation for homogeneous convex objects. The effect of orientation is investigated by rotating the upright disk ($ka = 12.56$) of Sec. IV A

clockwise by 18° and 34°, respectively, about the y axis. This places the zero of the scatter function at the horizontal, as can be seen by the inspection of Fig. 5, so that the scatter function experiences a phase change about the horizontal. The difference between the scattered field and sonar equation for the two rotated cases is almost identical to the unrotated case shown in Figs. 2(a)–(c). The variation across the cases
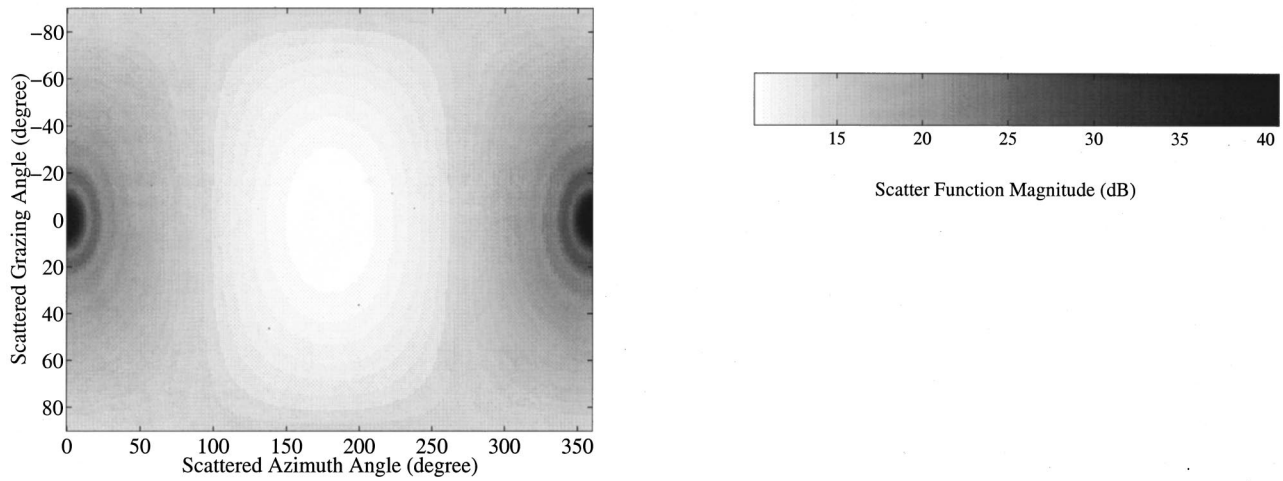
FIG. 12. Similar to Fig. 4, but for a pressure-release prolate spheroid of aspect ratio 2 with a major axis of 40 m and a minor axis of 20 m at 300 Hz. The forward scatter direction is along the major axis. At the bow aspect of the spheroid, $ka = 12.6$. The scatter function for the spheroid is given by Eq. (11.38) of Ref. 14.
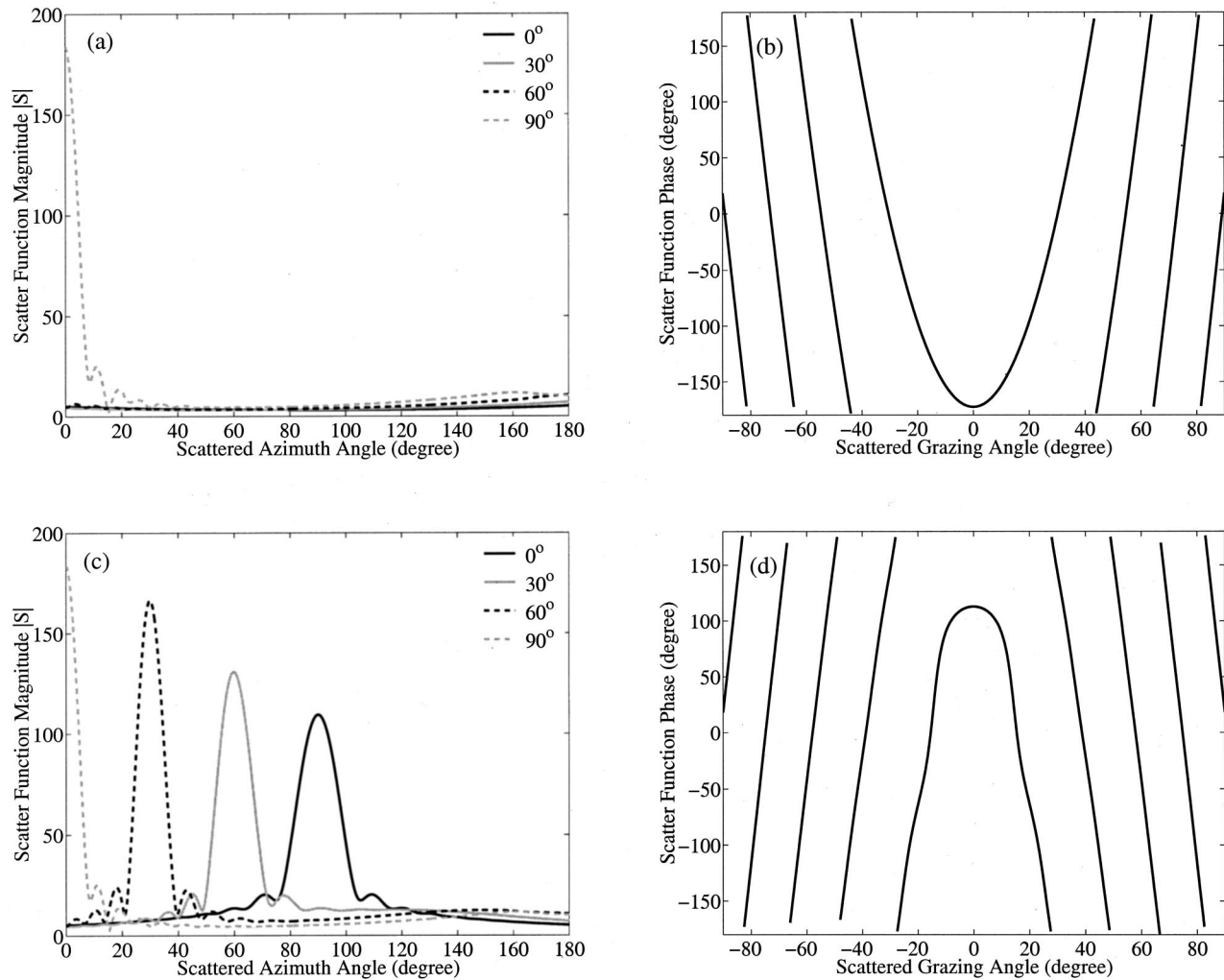

FIG. 13. Similar to Figs. 10(a)–(d) but for a pressure-release prolate spheroid of aspect ratio 2 with a major axis of 40 m and a minor axis of 20 m at 300 Hz. The forward scatter direction is along the major axis. At the bow aspect of the spheroid, $ka = 12.6$. The solid curves in (a) and (c) for $(\alpha_i - 90°) = 0°$ are slices through Fig. 12 at the back $\beta = 180°$, and forward $\beta = 0°$ scatter azimuths, respectively, of the scattered plane waves. The width λ/L of the scatter function main lobe at horizontal grazing incidence $[(\alpha_i - 90°) = 0°]$ is 14.3° or 0.25 rad in (c).

is less than roughly 1 dB for ranges beyond 1 km, showing that the condition $2\Delta\psi < \lambda/L$, as shown in Fig. 2(d), holds, regardless of object orientation. This makes sense because the condition states that the sonar equation will be a good approximation if the scatter function undergoes no more than one oscillation within $\pm\Delta\psi$. This minimizes the destructive interference possible in multimodal propagation and scattering.

There are two limiting object shapes for homogeneous convex objects, flat and rounded ones. Flat objects, such as the disk examined in the previous section, are highly directional scatterers when ka is large. In free space, they scatter the strongest in specular and forward scatter directions. The sonar equation is only valid for flat objects when the condition $2\Delta\psi < \lambda/L$ holds, as demonstrated in the previous section for an upright disk and in this section for the rotated disk. We note that the scattered field level in the forward azimuth is identical to that given in the back azimuth in Figs. 2, 3, and 6 because the scatter function for the upright disk is antisymmetric about the plane of the disk, as can be seen in Eq. (24) and Fig. 4. The phase of the scatter function is constant over the main lobe, as can be seen in Eq. (24). This constancy over the main lobe is characteristic of flat objects, where the narrowest lobe is always the main lobe for broadside incidence. Rectangular plate examples are investigated in Ref. 15.

When the condition $2\Delta\psi < \lambda/L$ does not hold, the sonar equation can still be extremely accurate in nonforward scatter azimuths for spheres and certain other rounded or smoothly varying convex objects. For these objects, the scatter function is approximately uniform in nonforward directions but has a main lobe in the forward direction of width λ/L. This uniformity makes it possible to approximate the scatter function in nonforward azimuths as a factorable constant over $\pm\Delta\psi$, making the sonar equation valid. The sonar equation, however, will still only be valid in the forward scatter azimuth for spheres and rounded objects when $2\Delta\psi < \lambda/L$ holds because they behave like flat objects in forward scatter by Babinet's principle. These issues will be illustrated for two smoothly varying convex objects, the sphere and the prolate spheroid, in the same three waveguides examined in previous sections. Babinet's principle will be discussed further in Sec. V.

As expected, the sonar equation predicts the backscattered field much more accurately than the forward scattered field for both the sphere and the prolate spheroid, as shown in Figs. 8 and 11, respectively, for the various waveguides. This can be explained by examining the scatter function of a sphere, given in Ref. 14 and plotted in Figs. 9 and 10. Figure 10(a) shows that the magnitude of the scatter function in the backscatter azimuth for the sphere is approximately constant over $\pm\Delta\psi$ in the Pekeris silt and sand waveguides, where $\Delta\psi$ can be determined from Fig. 2(d). Figure 10(b) shows that the phase of the scatter function varies by less than $\pi/4$ over $\pm\Delta\psi$ and so can be considered effectively constant. This means that the scatter function can be factored from the modal sum in Eq. (1) so that propagation is decoupled from scattering. The sonar equation then becomes valid in the
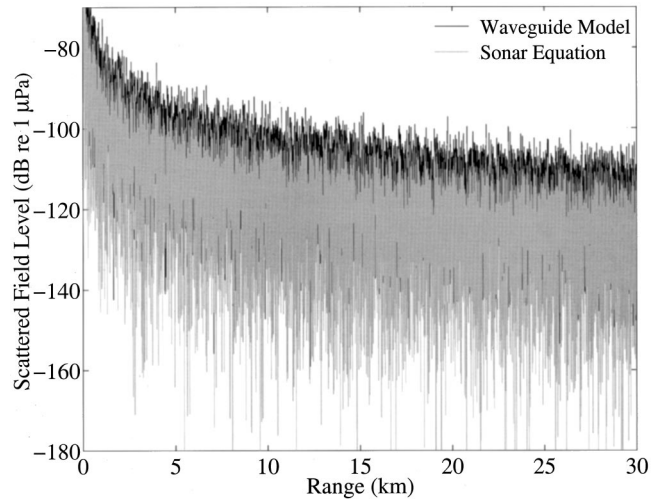

FIG. 14. Similar to Fig. 11(e), but for a pressure-release prolate spheroid of aspect ratio 5 with a major axis of 20 m and a minor axis of 4 m at 300 Hz. The spheroid is aligned such that the incoming plane waves are incident at the bow aspect where $ka = 2.5$.

backscatter direction for the sphere in the Pekeris sand and silt waveguides.

In the perfectly reflecting waveguide, $\Delta\psi$ is $\pi/2$ rad or 90°. In this case, some higher-order modes at very steep incident grazing angles near 90°, for example, scatter much stronger in the backscatter azimuth than the other modes of lower order that scatter more uniformly, as shown in Fig. 10(a). The phase of the scatter function also varies by more than 180° over $\Delta\psi$. As a result, scattering is not completely decoupled from propagation and so the sonar equation provides only a crude approximation in the backscatter azimuth, as shown in Fig. 8(e).

In the forward azimuth, the sphere scatters approximately as a flat object with the same projected area, by Babinet's principle, and so behaves like the disk of Fig. 2. Similar conclusions can be drawn for the prolate spheroid from Figs.
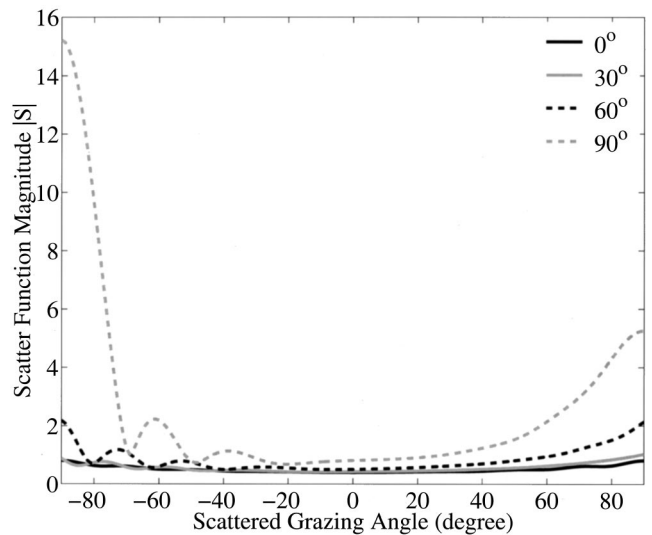

FIG. 15. Similar to Fig. 5 but for a pressure-release prolate spheroid of aspect ratio 5 with a major axis of 20 m and a minor axis of 4 m at 300 Hz in the backscatter azimuth $\beta = 180°$. The forward scatter direction is along the major axis. At the bow aspect of the spheroid, $ka = 2.5$.
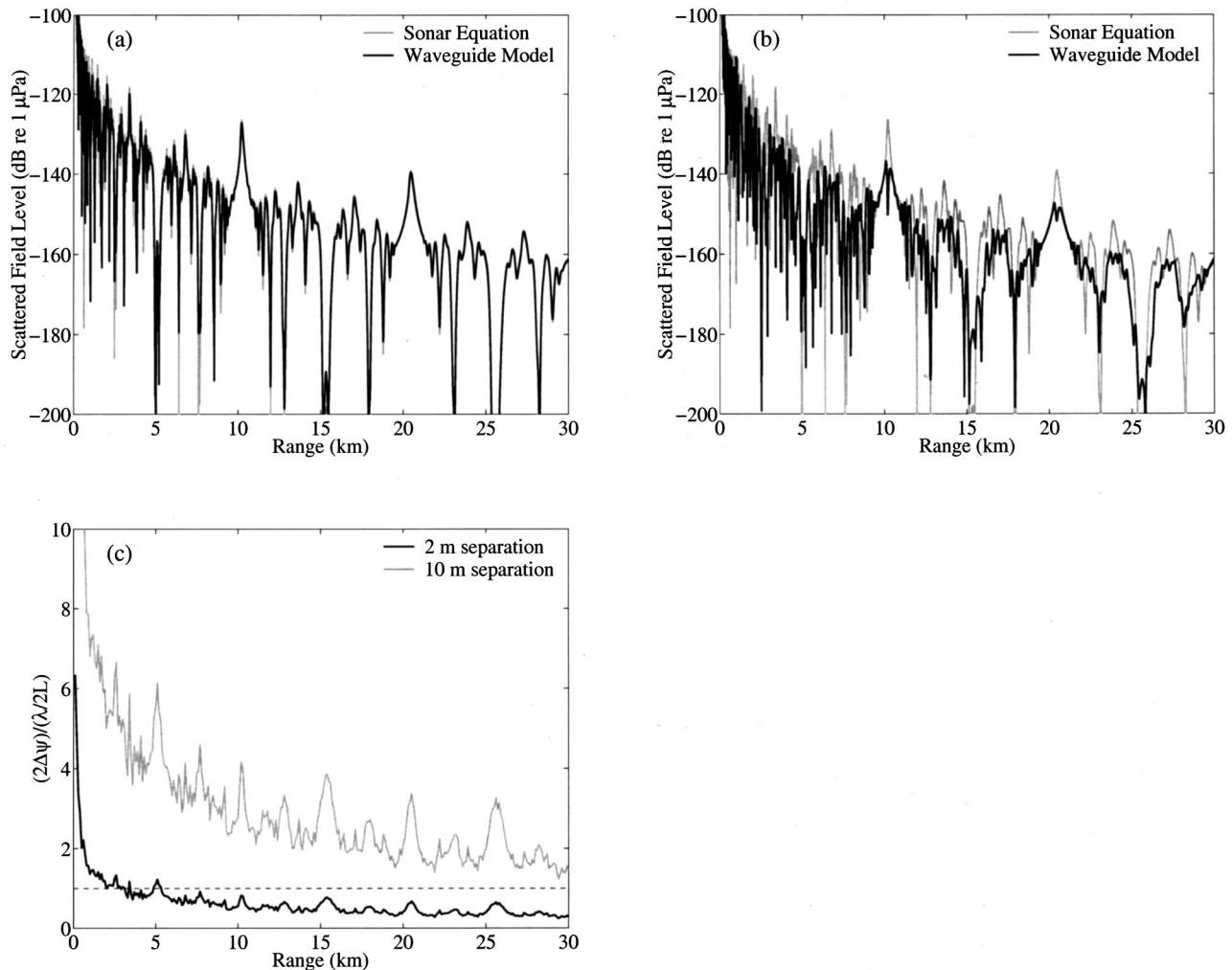
FIG. 16. Similar to Fig. 2(a) but for a "single object" comprised of two point scatterers with a separation of (a) $L = 2$ m and (b) $L = 10$ m, respectively, at 1500 Hz. (c) The ratio $2\Delta\psi/(\lambda/2L)$ for the examples given in (a) and (b). The sonar equation provides a good approximation to the scattered field in the waveguide when $2\Delta\psi/(\lambda/2L) < 1$.

11–13. Its scatter function is given in Ref. 14.

The sonar equation can sometimes underestimate the scattered field depending on the object type, size, waveguide, and frequency. In Fig. 14, the sonar equation underestimates the backscattered field from a spheroid in a perfectly reflecting waveguide by a small amount, roughly 3 dB. The sonar equation assumes that the scatter function is constant and equal to that at the incident $(\pi/2 - \alpha_i) = 0$ and scattered $(\pi/2 - \alpha) = 0$ grazing angles in Fig. 15. This, however, corresponds to the backscatter minimum in the scatter function plot and is not representative of all values within $\pm\Delta\psi$.

D. Nonconvex objects and fluctuating objects

The scatter function lobes for homogeneous convex objects have minimum widths limited to λ/L by diffraction. For more general, potentially inhomogeneous, and nonconvex objects, the scatter function lobes are limited by both diffraction and interference from different parts of the object. For example, a situation may arise where it is convenient to consider an aggregate of disjoint scatterers as a "single object" with a single scatter function. In the limiting case of two point scatterers separated by length L normal to the incident wave, the main lobe of this "single object's" scatter function has the narrowest width possible $\lambda/(2L)$. The condition for the sonar equation to become valid in a waveguide then is the most stringent $2\Delta\psi < \lambda/2L$.

The scatter function for a "single object" comprised of two point scatterers separated in depth by length L is $2\cos(\pi L[\cos\alpha_i - \cos\alpha]/\lambda)$ if the scatter function of each point is unity. The field scattered from this "single object" is given in Figs. 16(a) and (b) for point separations of $L = 2$ m and $L = 10$ m, respectively, at 1500 Hz using both the sonar equation and waveguide scattering model. For $L = 2$ m the sonar equation is valid and matches the waveguide model because the condition $2\Delta\psi < \lambda/2L$ is satisfied, as can be seen in Fig. 16(c). This condition is not satisfied for the $L = 10$ m case, where the sonar equation is not valid, as can be seen in Figs. 16(b) and (c).

For an object whose orientation is unknown or constantly varying, like a fluctuating target, a conservative cri-

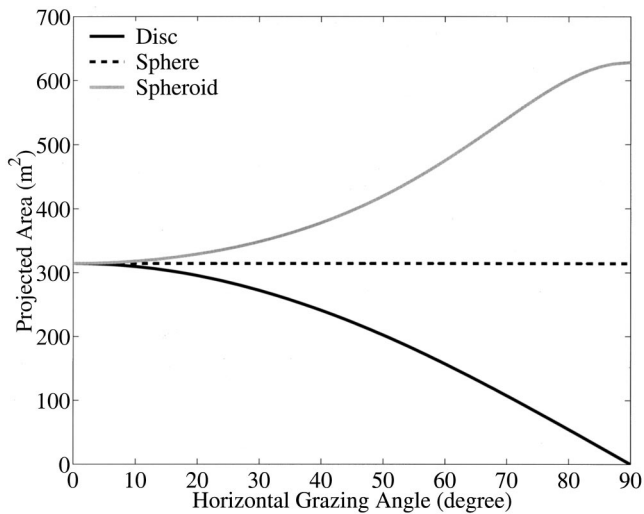Ratilal *et al.*: Sonar equation and Babinet's principle in a stratified medium

FIG. 17. Projected areas of a 10 m radius rigid circular disk, a 10 m radius pressure-release sphere and a pressure-release prolate spheroid of aspect ratio 2 with a major axis of 40 m and a minor axis of 20 m are plotted as a function of horizontal grazing angle $|\alpha_i - 90°|$ of the incident plane waves. The orientation of the disk and spheroid are similar to Figs. 2 and 11.

terion for the sonar equation's validity in a waveguide is $2\,\Delta\psi < \lambda/2L_{max}$ where L_{max} is the largest spatial extent of the object, which may be composed of an aggregate of disjoint scatterers.

E. Forward scatter function and projected area for homogeneous convex objects

According to the extinction or forward scatter theorem in free space,[10,13,16] the scatter function of an object in the forward direction at a given frequency is proportional to the object's projected area normal to the direction of propagation of the incident wave for high ka. The projected area of the 10 m radius rigid circular disk is largest for plane waves incident on the disk at horizontal grazing $[(\pi/2-\alpha_i)=0]$, as shown in Figs. 5 and 7(a). At other incident grazing angles, the projected area of the disk is smaller and the peak value of the scatter function corresponding to forward scatter decreases. In addition, the width of the forward scatter lobe broadens since it is inversely related to the projected area. For a compact pressure-release object ($ka \ll 1$) the scatter function becomes omnidirectional.
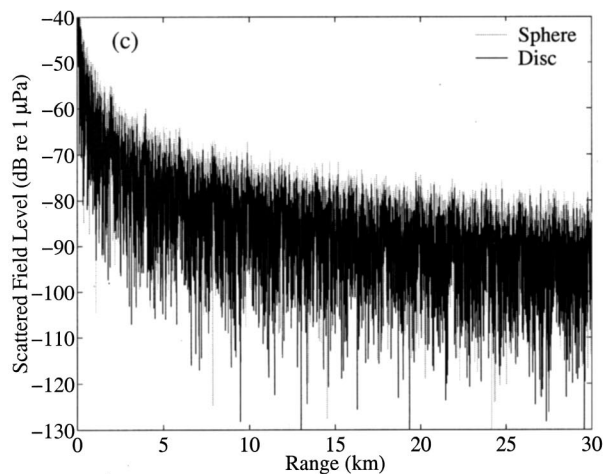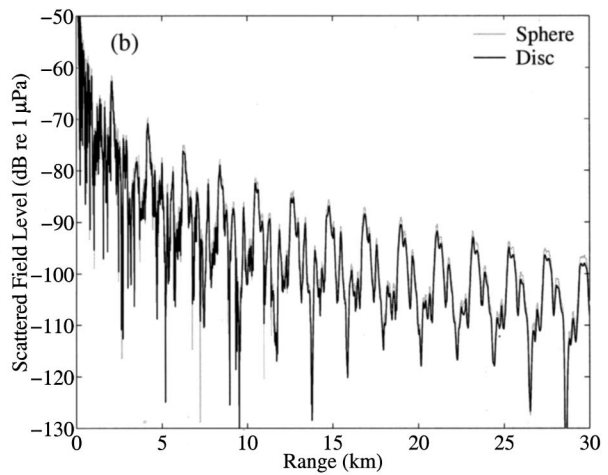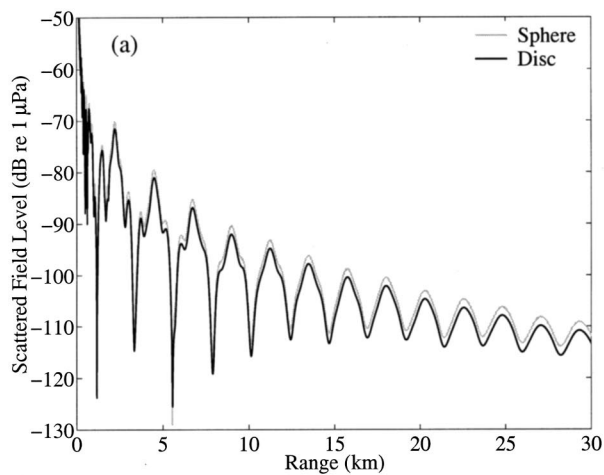

FIG. 18. The forward scattered field at 300 Hz calculated using the waveguide scattering model, Eq. (1), from a 10 m radius pressure release sphere is compared to that from a rigid circular disk of radius 10 m in (a) Pekeris silt, (b) Pekeris sand, and (c) perfectly reflecting waveguides. ka is 12.6 for these examples. The geometry of the setup is similar to Figs. 2 and 8, except that the receiver is in the forward azimuth.
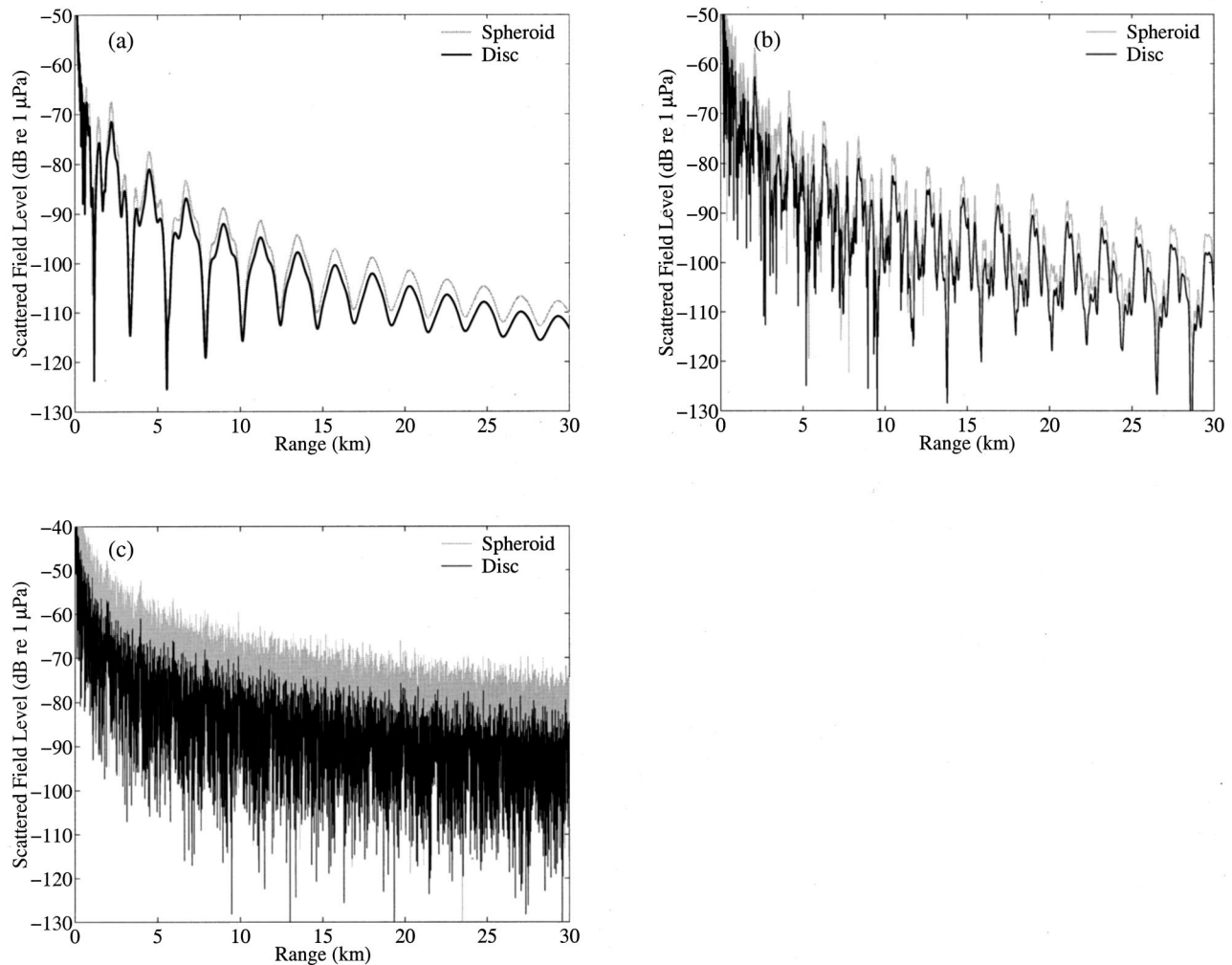
FIG. 19. Similar to Figs. 18(a)–(c) but for a pressure-release prolate spheroid of aspect ratio 2 with a major axis of 40 m and a minor axis of 20 m and a rigid circular disk of radius 10 m. ka is 12.6 for the disk and for the spheroid in the bow aspect in these examples. The geometry of the setup is similar to Figs. 2 and 11, except that the receiver is in the forward azimuth.

For the 10 m radius pressure-release sphere in Fig. 10(c), the forward scatter function's peak is constant because the projected area of the sphere is independent of the angle of incidence. This is not true for the pressure-release prolate spheroid in Fig. 13(c), where the projected area increases with the incident grazing angle. This causes the scatter function to have a forward scatter lobe with increasing peak amplitude and decreasing width.

V. BABINET'S PRINCIPLE AND FORWARD SCATTERED FIELD IN A WAVEGUIDE

Babinet's principle maintains that the forward scattered fields from impenetrable objects in free space with identical projected areas are equal for large ka.[10,13] This also holds true for some penetrable objects.[10] The forward scattered field from a large object in free space interferes destructively with the incident field to form a shadow directly behind the object. In the farfield, the intensity of the forward scattered field is the same pattern as that diffracted through a hole of the same projected area as the object in a rigid wall. The forward scattered field then only depends on the projected area of the object. It is therefore possible to replace the 3-D object by the largest 2-D cross section of the object normal to the incident wave. This is Babinet's principle. For example, in free space, a sphere, and a circular disk of the same radius, with the disk aligned normal to the incident wave vector, have the same projected area, and hence identical forward scattered fields when $ka \gg 1$.

We find that Babinet's principle is approximately valid in forward *azimuth* in a waveguide if the projected area of the object does not vary significantly for incident plane waves over $\pm \Delta \psi$. We stress that this holds in the forward *azimuth* because there is generally no unique forward direction in a waveguide. This result is illustrated in Figs. 17–20. The projected areas for an upright disk, sphere, and prolate spheroid are shown as a function of horizontal grazing angle in Fig. 17, where the spheroid is oriented as in Sec. IV C. All three objects have the same projected area for a horizontally propagating plane wave. The spheroid deviates the most from its flat counterpart, the disk, as the grazing angle changes. The corresponding values of $\Delta \psi$ over range can be determined from Fig. 2(d) for the sand and silt waveguides, and are typically less than 30°, where the variation in projected area is small for all three objects. For the perfectly
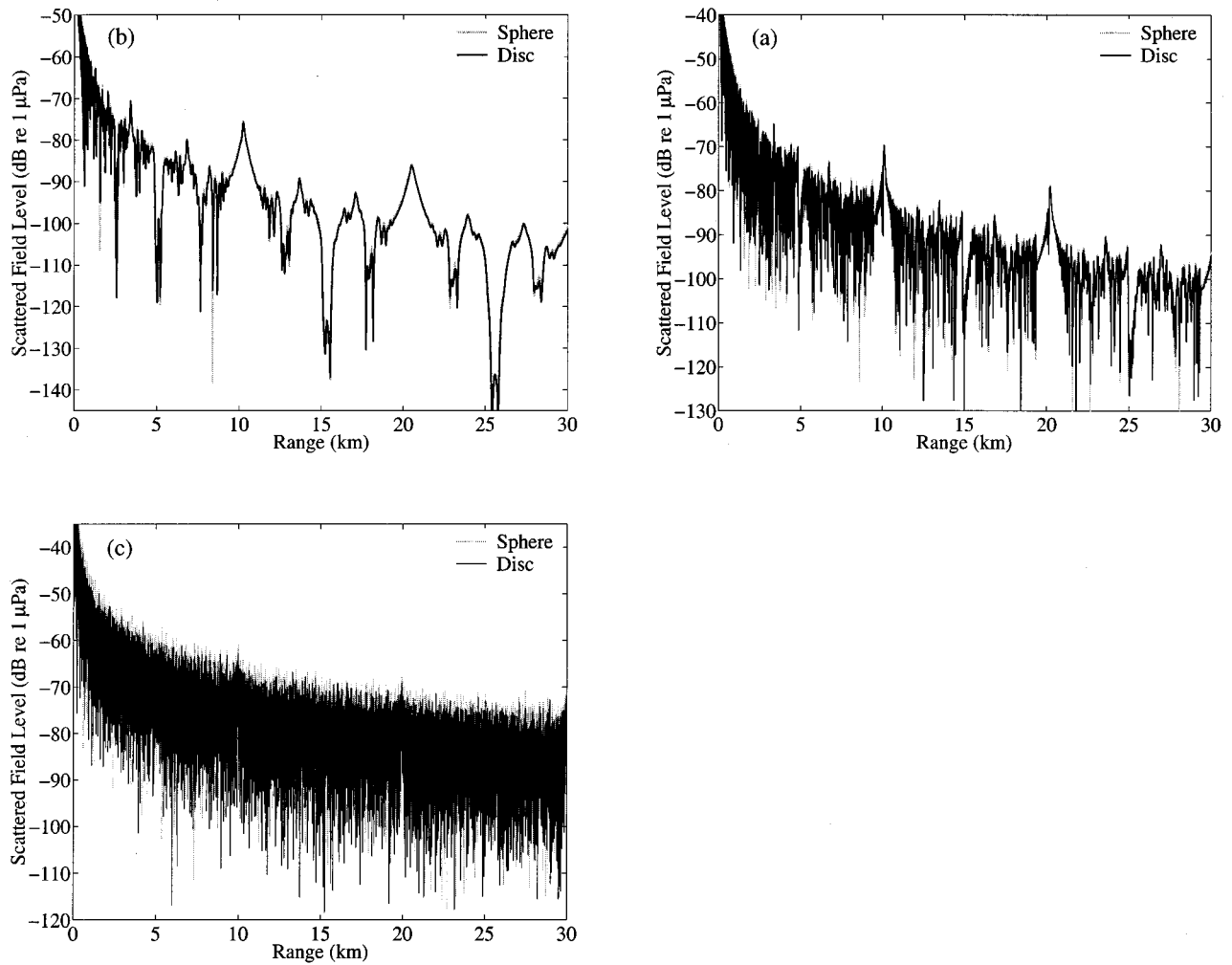
FIG. 20. Similar to Fig. 18 but at 1500 Hz. ka is 62.8 for these examples.

reflecting waveguide, the variation in projected area is very large for all three objects, since $\Delta\psi$ is 90°. Babinet's principle is then expected to be valid for these objects in the silt and sand waveguides at high ka, but not in the perfectly reflecting waveguide. This is found to be the case in Figs. 18–20, where in Figs. 18–19 ka is not large enough for Babinet's principle to provide a better than crude approximation, even in freespace. (The spheroid's scatter function is computed using spheroidal wave functions that are known to be numerically unstable for large arguments[17] and so the scattered field at the higher ka value of 62.8 for the spheroid is not shown.)

When Babinet's principle holds in a waveguide, the sonar equation will only be valid in the forward scatter azimuth if the condition $2\Delta\psi<\lambda/2L$ is satisfied, regardless of object shape. This means that rounded objects such as spheres have no advantage over flat objects in attaining the sonar equation in the forward azimuth in a waveguide.

VI. CONCLUSION

As a general conclusion, we find that *the sonar equation is valid when the target's scatter function is roughly constant over the equivalent horizontal grazing angles $\pm\Delta\psi$ spanned by the dominant waveguide modes*. This is approximately true (1) for all objects when $2\Delta\psi<\lambda/2L$ and (2) for spheres and certain other rounded objects in nonforward scatter azimuths, even when (1) does not hold. For homogeneous convex objects condition (1) is the less stringent $2\Delta\psi<\lambda/L$.

The sonar operator has the ability to lower the frequency of transmission until the target's scatter function becomes approximately constant over $\pm\Delta\psi$. The sonar equation then becomes valid when $f<c/(4L\,\Delta\psi)$. Operating in this frequency regime is desirable because when the sonar equation is valid, only a single-parameter, target strength, is necessary to characterize the scattering properties of the target. This greatly simplifies target classification in a shallow water waveguide by making the traditional approach[1,2] valid.

We find that Babinet's principle is approximately valid in the forward *azimuth* in a waveguide if the projected area of the object does not vary significantly for incident plane waves over $\pm\Delta\psi$. When Babinet's principle holds in a waveguide, the sonar equation will only be valid in the forward scatter azimuth if the condition $2\Delta\psi<\lambda/2L$ is satisfied regardless of object shape. This means that rounded objects such as spheres have no advantage over flat objects in attain-

ing the sonar equation in the forward azimuth in a waveguide.

[1] R. J. Urick, *Principles of Underwater Sound* (McGraw-Hill, New York, 1983).

[2] National Defence Research Committee, *Physics of Sound in the Sea* (Peninsula, Los Altos, 1989).

[3] F. B. Jensen, W. A. Kuperman, M. B. Porter, and H. Schmidt, *Computational Ocean Acoustics* (American Institute of Physics, Woodbury, NY, 1994).

[4] W. S. Burdic, *Underwater Acoustic System Analysis* (Prentice–Hall, Englewood Cliffs, NJ, 1991).

[5] L. E. Kinsler, A. R. Frey, A. B. Coppens, and J. V. Sanders, *Fundamentals of Acoustics* (Wiley, New York, 1982).

[6] N. C. Makris and P. Ratilal, "Validity of the sonar equation and Babinet's principle for object scattering in a shallow water waveguide," J. Acoust. Soc. Am. **106**, 2158 (1999).

[7] F. Ingenito, "Scattering from an object in a stratified medium," J. Acoust. Soc. Am. **82**, 2051–2059 (1987).

[8] N. C. Makris and P. Ratilal, "A unified model for reverberation and submerged object scattering in a stratified ocean waveguide," J. Acoust. Soc. Am. **109**, 909–941 (2001).

[9] N. C. Makris, "A spectral approach to 3-D object scattering in layered media applied to scattering from submerged spheres," J. Acoust. Soc. Am. **104**, 2105–2113 (1998); **106**, 518 (1999) (Erratum).

[10] H. C. van de Hulst, *Light Scattering by Small Particles* (Dover, New York, 1981).

[11] N. C. Makris, F. Ingenito, and W. A. Kuperman, "Detection of a submerged object insonified by surface noise in an ocean waveguide," J. Acoust. Soc. Am. **96**, 1703–1724 (1994).

[12] P. M. Morse and K. U. Ingard, *Theoretical Acoustics* (Princeton University Press, Princeton, NJ, 1986), pp. 418–436.

[13] M. Born and E. Wolf, *Principles of Optics, Electromagnetic Theory of Propagation Interference and Diffraction of Light*, 6th ed. (Cambridge University Press, Cambridge, 1980).

[14] J. J. Bowman, T. B. A. Senior, and P. L. E. Uslenghi, in *Electromagnetic and Acoustic Scattering by Simple Shapes* (North-Holland, Amsterdam, 1969).

[15] P. Ratilal, "Remote sensing of submerged objects and geomorphology in continental shelf waters with acoustic waveguide scattering," Ph.D. thesis, MIT, Cambridge, MA, 2002.

[16] P. Ratilal and N. C. Makris, "Extinction theorem for object scattering in a stratified medium," J. Acoust. Soc. Am. **110**, 2924 (2001).

[17] S. Asano, "Light scattering properties of spheroidal particles," Appl. Opt. **18**, 712–723 (1979).